Supporting Information

Influence of terminal halogen moieties on the phase structure of short-core achiral hockey-stick shaped mesogens: Design, synthesis and structure-property relationship

Supreet Kaur,[a] Golam Mohiuddin,[a] Pragnya Satapathy,[b] Rajib Nandi,[a] Vidhika Punjani,[a] S. Krishna Prasad,[b] Santanu Kumar Pal*[a]

[a]Department of Chemical Sciences, Indian Institute of Science Education and Research (IISER) Mohali, Sector-81, SAS Nagar, Knowledge City, Manauli-140306, India.
E-mail: skpal@iisermohali.ac.in

[b]Centre for Nano and Soft Matter Sciences, Jalahalli, Bengaluru, India.

Table of contents

1. Synthesis:

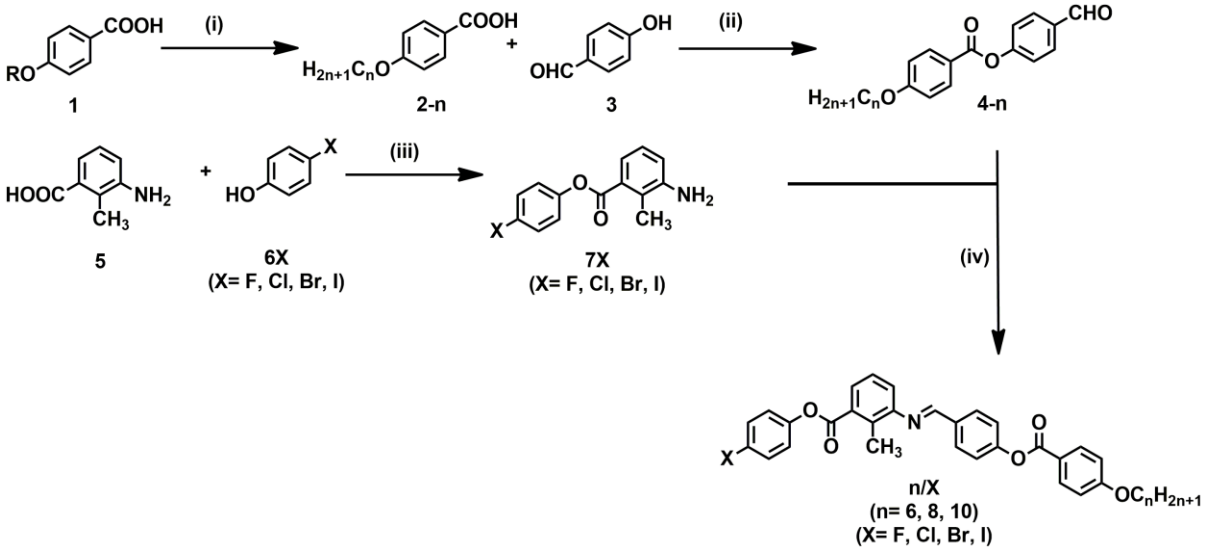

Synthetic details of the compounds, Reagents and conditions: **(i)** $C_nH_{2n+1}Br$, KOH-EtOH, 6h, KOH-H_2O, 3h; **(ii)** DCC, DMAP, Dry DCM, 24 h; **(iii)** DCC, DMAP. Dry DCM, 24 h; **(iv)** absolute EtOH glacial AcOH, reflux, 4h.

Figure S1: Synthetic scheme for the target compounds **n/X**.

Step 1:

In refluxing conditions, an ethanolic solution of 4-Hydroxybenzoic acid **1** (1 eq.) was mixed with potassium hydroxide (KOH) (2.5 eq.) solution with further addition of 1-Bromohexane (1.2 eq.). After 6 hours of stirring, for base hydrolysis, 10% KOH was added and refluxed for another 3 hours. The reaction mixture was then poured in acid water for neutralisation. The white solid appeared on constant stirring and was filtered and collected as the product **2-6**. Yield: 85 %

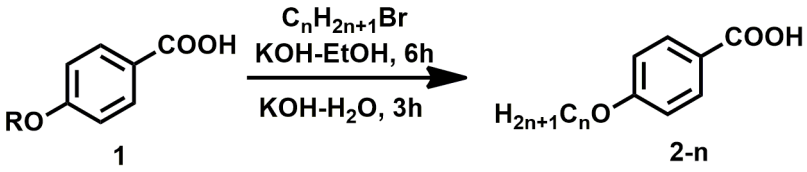

The other homologues with varying the number of carbon atoms (n) in the alkoxy chain (n= 6, 8, 10) i.e. **2-6**, **2-8** and **2-10** were synthesized following the above procedure with appropriate amount of alkyl bromides.

Step 2:

4-(octyloxy)benzoic acid **2-8** (1 eq.) was dissolved in dry dichloromethane (DCM) in an inert nitrogen atmosphere followed by addition of N,N'-Dicyclohexylcarbodiimide (DCC) (1.2 eq.) and catalytic amount of 4-dimethylaminopyridine (DMAP). 4-Hydroxybenzaldehyde **3** (1 eq.) was added after half an hour of stirring. The reaction mixture was stirred for 24 hours at room temperature. The precipitate of Dicyclohexylurea (DCU) was removed by filtration and the solvent DCM was evaporated to get the crude product. It was purified by column chromatography using silica (100-200 mesh) eluting with a mixture of hexane-ethyl acetate. The product **4-8** was obtained as a white solid. Yield: 65 % ; ^{1}H NMR (400 MHz, $CDCl_3$, δ in ppm): δ = 10.05 (s, 1H, -CHO), 8.22-8.16 (m, 2H, Ar-H), 7.99 (d, 2H, *J* = 8.0 Hz, Ar-H), 7.43 (d, 1H, *J* = 8.0 Hz, Ar-H), 7.36 (d, 1H, *J* = 8.0 Hz, Ar-H), 7.01 (d, 2H, *J* = 8.0 Hz, Ar-H), 4.08 (t, 2H, *J* = 6.0 Hz, -OCH_2-), 1.89-1.82 (m, 2H, -CH_2-), 1.54-1.47 (m, 2H, - CH_2-), 1.37-1.32 (m, 8H, - $(CH_2)_4$-), 0.92 (t, 3H, *J* = 6.0 Hz, -CH_3); ^{13}C NMR (100 MHz, $CDCl_3$, δ in ppm): δ = 14.14, 22.68, 25.99, 29.09, 29.22, 29.34, 31.82, 68.41, 114.44, 120.79, 122.63, 131.26, 132.45, 133.88, 155.92, 163.88, 164.27, 191.05.

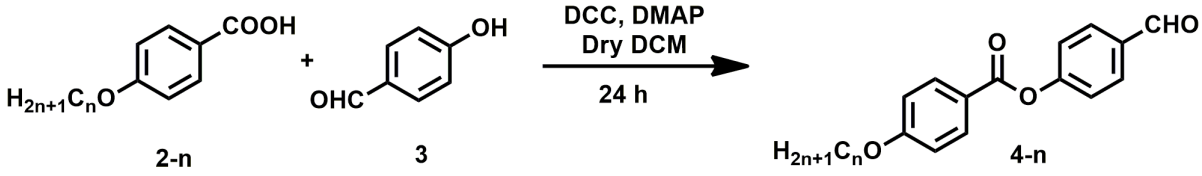

Using the same procedure, other compounds **4-6**, **4-8** and **4-10** were prepared.

Compound	**M+H**	**M-H**	**Exact Mass**	**Observed Mass**	**% error**
4-8	355.1909	353.1753	354.1831	355.0863	0.000294

Step 3:

3-Amino-2-methylbenzoic acid **5** (1 eq.) was dissolved in dry dichloromethane (DCM) in an inert nitrogen atmosphere followed by addition of N,N'-Dicyclohexylcarbodiimide (DCC) (1.2 eq.) and catalytic amount of 4-dimethylaminopyridine (DMAP). 4-Bromophenol **6Br** (1 eq.) was added after half an hour of stirring. The reaction mixture was stirred for 24 hours at room temperature. The precipitate of Dicyclohexylurea (DCU) was removed by filtration and the solvent DCM was evaporated to get the solid crude product. The solid was recrystallized 2-3 times using absolute ethanol to give pure product **7Br**. Yield: 85 % ; ^{1}H NMR (400 MHz, $CDCl_3$, δ in ppm): δ = 7.56 (d, 2H, *J* = 8.0 Hz, Ar-H), 7.51 (d, 1H, *J* = 8.0 Hz, Ar-H), 7.18-7.12 (m, 3H, Ar-H), 6.93 (d, 1H, *J* = 8.0 Hz, Ar-H), 3.82 (s, 2H, -NH_2), 2.45 (s, 3H, -CH_3); ^{13}C NMR (100 MHz, $CDCl_3$, δ in ppm): δ = 13.90, 118.88, 119.17, 121.08, 123.64, 124.07, 126.26, 129.88, 132.52, 145.77, 150.02, 166.40.

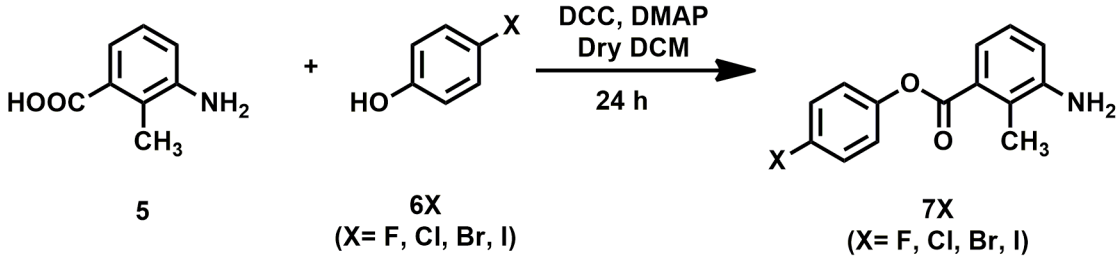

Using the same procedure, other compounds **7F**, **7Cl**, **7Br** and **7I** were prepared.

Compound	**M+H**	**M-H**	**Exact Mass**	**Observed Mass**	**% error**
7Br	306.0129	303.9973	305.0051	306.0121	0.000261

Step 4:

The final Schiff base compounds (**n/X**) were prepared by refluxing a mixture of ethanolic solution of **4-8** (1 eq.) with **7Br** (1 eq.) and a few drops of glacial acetic acid as catalyst for 4 h. The precipitated product was dissolved in hot boiling ethanol and the insoluble white solid was collected as the pure product **8/Br**. Yield: 78 % ; ^{1}H NMR (400 MHz, $CDCl_3$, δ in ppm): δ = 8.39 (s, 1H, -CH=N-), 8.18 (d, 2H, *J* = 8.0 Hz, Ar-H), 8.03 (d, 2H, *J* = 8.0 Hz, Ar-H), 7.97 (d, 1H, *J* = 8.0 Hz, Ar-H), 7.58 (d, 2H, *J* = 8.0 Hz, Ar-H), 7.39-7.35 (m, 3H, Ar-H), 7.17-7.15 (m, 3H, Ar-H), 7.01 (d, 2H, *J* = 8.0 Hz, Ar-H), 4.08 (t, 2H, *J* = 6.0 Hz, -OCH_2-), 2.67 (s, 3H, -CH_3), 1.89-1.82 (m, 2H, -CH_2-), 1.54-1.47 (m, 2H, -CH_2-), 1.37-1.33 (m, 8H, -$(CH_2)_4$-), 0.92 (t, 3H, *J* = 8.0 Hz, -CH_3); ^{13}C NMR (100 MHz, $CDCl_3$, δ in ppm): δ = 14.13, 15.37, 22.68, 26.01, 29.11, 29.25, 29.35, 31.83, 68.40, 114.39, 118.96, 121.12, 122.37, 122.40, 123.64, 126.41, 127.98, 129.67, 130.13, 132.40, 132.55, 133.65, 134.59, 148.67, 152.49, 153.72, 159.42, 163.75, 164.63, 166.83; FT-IR (ν_{max} in cm^{-1}): 1606 ($\nu_{CH=N}$, imine), 1731 ($\nu_{C=O}$, ester), 2922 (ν_{C-H}, alkanes); UV-vis (nm): 276 nm, 330 nm.

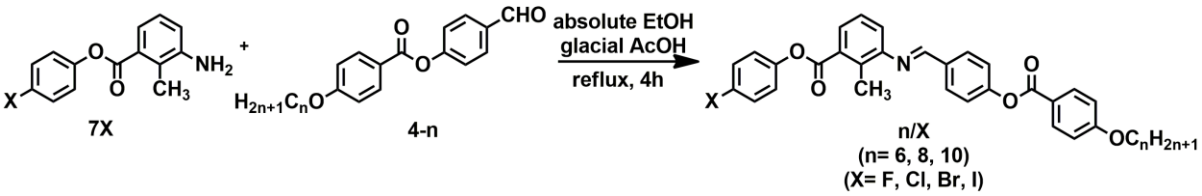

Compound	M+H	M-H	Exact Mass	Observed Mass	% error
8/Br	642.1855	640.1699	641.1777	642.1839	0.000249

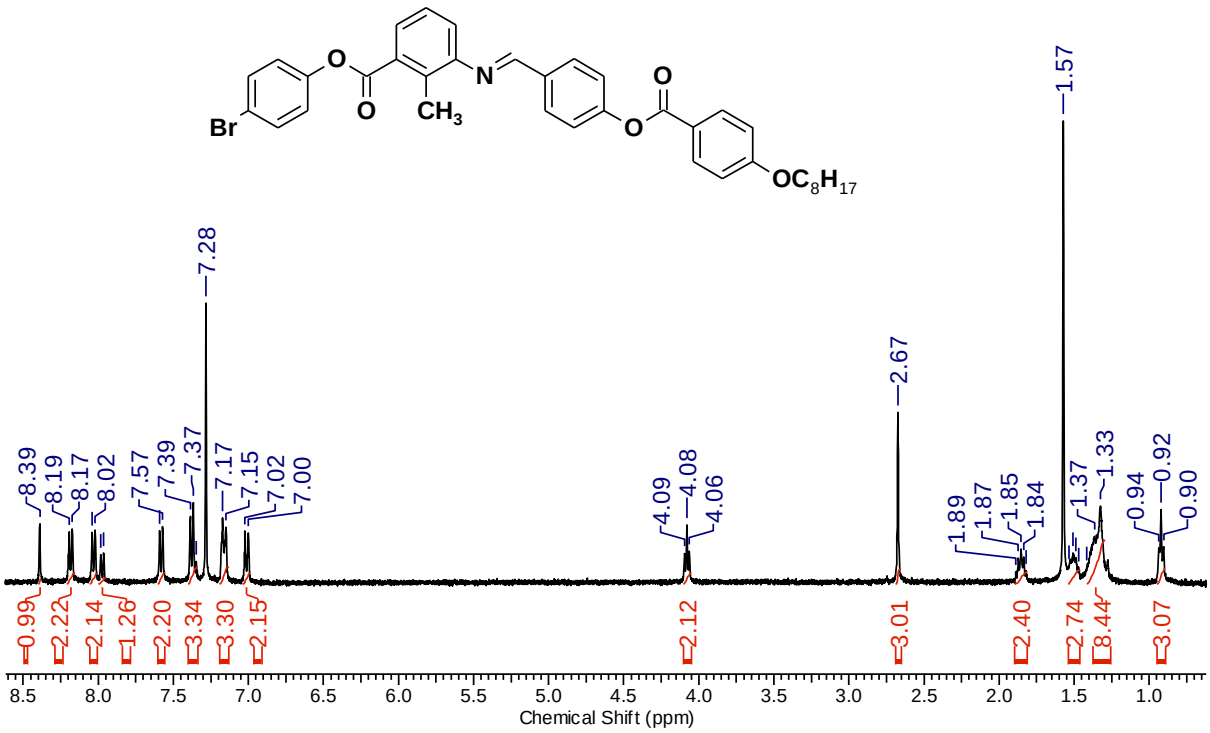

Figure S2: ^{1}H NMR of compound **8/Br**.

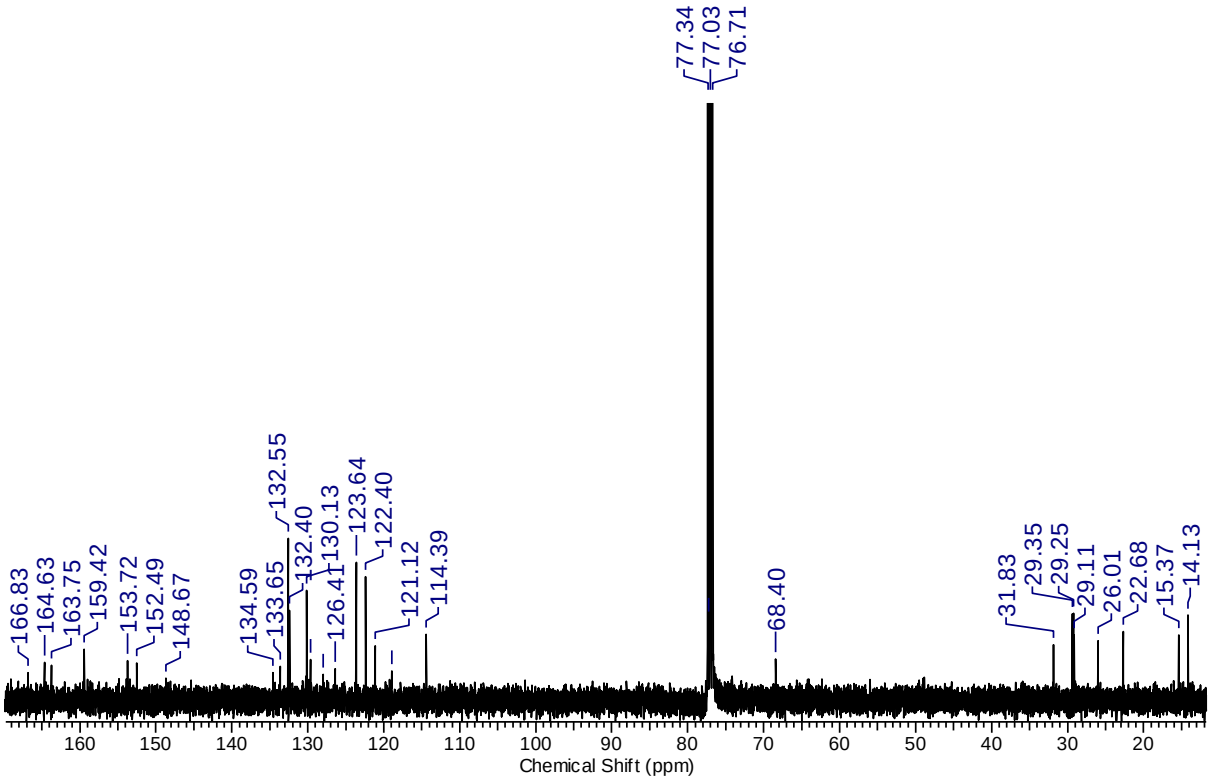

Figure S3: ^{13}C NMR of compound **8/Br**.

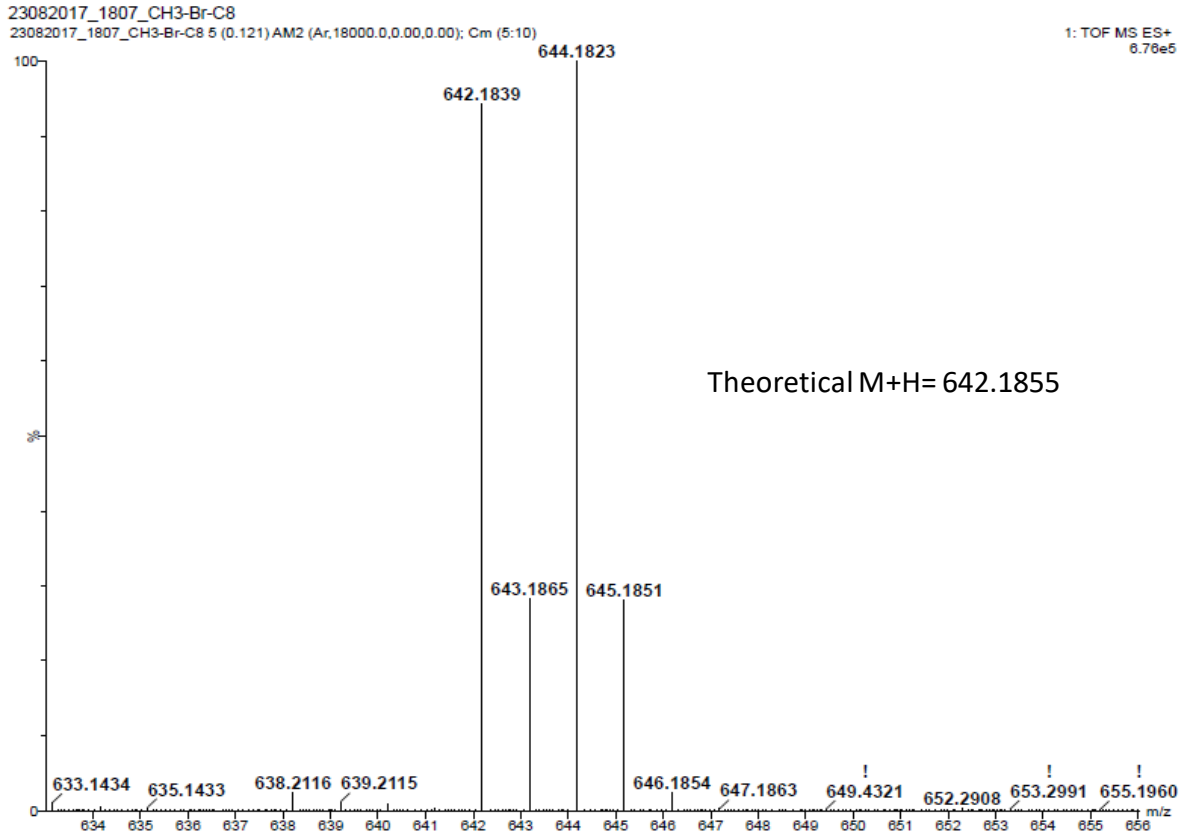

Figure S4: ESI spectrum of compound **8/Br**.

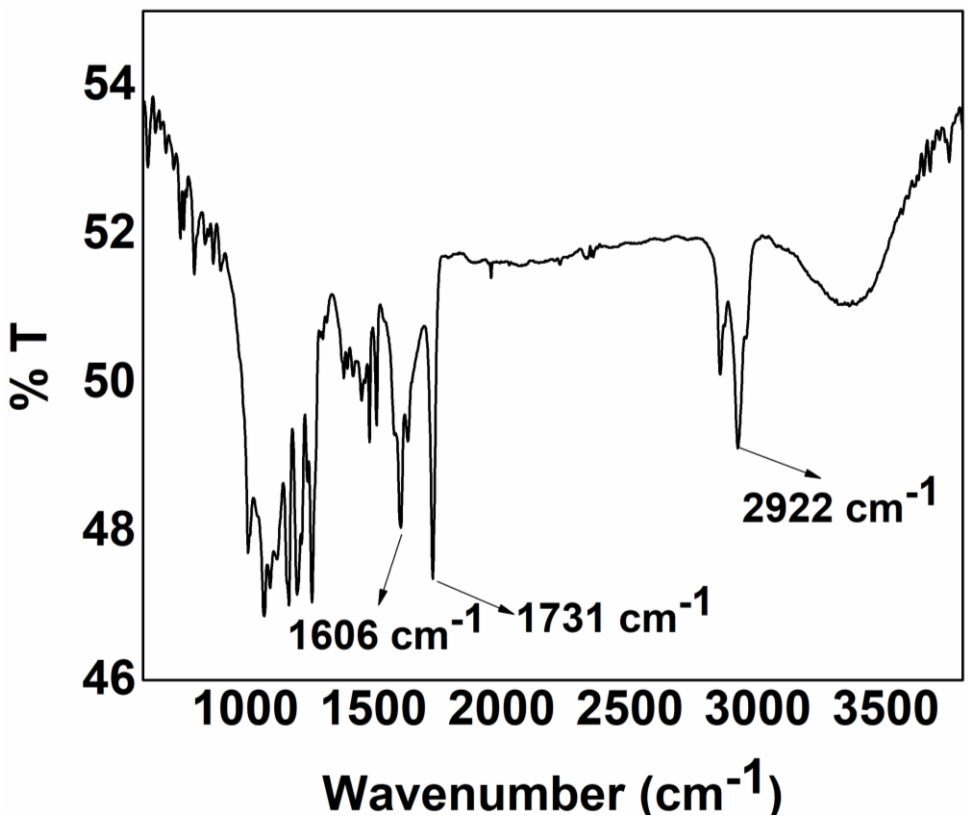

Figure S5: FT-IR spectrum of compound **8/Br**.

Characterization:

Compound **4-6**:

^{1}H NMR (400 MHz, $CDCl_3$, δ in ppm): δ = 10.05 (s, 1H, -CHO), 8.23-8.16 (m, 3H, Ar-H), 7.99 (d, 1H, *J* = 8.0 Hz, Ar-H), 7.44-7.23 (m, 2H, Ar-H), 7.01 (d, 2H, *J* = 8.6 Hz, Ar-H), 4.08 (t, 2H, *J* = 6.6 Hz, -OCH_2-), 1.89-1.82 (m, 2H, -CH_2-), 1.55-1.28 (m, 6H, -$(CH_2)_3$-), 0.95 (t, 3H, *J* = 6.4 Hz, -CH_3).

^{13}C NMR (100 MHz, $CDCl_3$, δ in ppm): δ = 14.06, 22.61, 25.67, 29.06, 31.56, 68.40, 114.44, 122.03, 122.64, 131.28, 131.88, 132.44, 155.50, 163.82, 170.41, 191.08.

Compound	M+H	M-H	Exact Mass	Observed Mass	% error
4-6	327.1596	325.1440	326.1518	327.1579	0.00052

Compound **4-10**:

^{1}H NMR (400 MHz, $CDCl_3$, δ in ppm): δ = 10.05 (s, 1H, -CHO), 8.17 (dd, 2H, *J* = 4.0, 8.0 Hz, Ar-H), 7.99 (d, 2H, *J* = 8.0 Hz, Ar-H), 7.43 (dd, 2H, *J* = 4.0, 8.0 Hz, Ar-H), 7.01 (d, 2H, *J* = 8.0 Hz, Ar-H), 4.07 (t, 2H, *J* = 6.0 Hz, -OCH_2-), 1.87-1.81 (m, 2H, -CH_2-), 1.52-1.47 (m, 2H, -CH_2-), 1.37-1.30 (m, 12H, - $(CH_2)_6$-), 0.91 (t, 3H, *J* = 8.0 Hz, -CH_3).

^{13}C NMR (100 MHz, $CDCl_3$, δ in ppm): δ = 14.15, 22.71, 25.99, 29.09, 29.34, 29.38, 29.57, 29.58, 31.91, 68.42, 114.44, 120.79, 122.64, 131.26, 132.45, 133.89, 155.93, 163.89, 164.27, 191.06.

Compound	M+H	M-H	Exact Mass	Observed Mass	% error
4-10	383.2222	381.2066	382.2144	383.2207	0.00039

Compound **7F**:

^{1}H NMR (400 MHz, $CDCl_3$, δ in ppm): δ = 7.52 (dd, 1H, *J* = 4.0, 8.0 Hz, Ar-H), 7.22-7.11 (m, 5H, Ar-H), 6.93 (dd, 1H, *J* =1.0, 7.9 Hz, Ar-H), 3.65 (s, 2H, -NH_2), 2.45 (s, 3H, -CH_3).

^{13}C NMR (100 MHz, $CDCl_3$, δ in ppm): δ = 13.91, 116.03, 116.26, 119.09, 121.05, 123.16, 123.24, 124.02, 126.25, 130.03, 145.76, 166.81.

Compound	M+H	M-H	Exact Mass	Observed Mass	% error
7F	246.093	244.0774	245.0852	246.0934	0.00016

Compound **7Cl**:

^{1}H NMR (400 MHz, $CDCl_3$, δ in ppm): δ = 7.51 (dd, 1H, *J* = 1.0, 7.8 Hz, Ar-H), 7.42 (dd, 2H, *J* = 2.1, 6.7 Hz, Ar-H), 7.20-7.14 (m, 3H, Ar-H), 6.93 (dd, 1H, *J* = 1.0, 7.8 Hz, Ar-H), 3.86 (s, 2H, -NH_2), 2.45 (s, 3H, -CH_3).

^{13}C NMR (100 MHz, $CDCl_3$, δ in ppm): δ = 13.90, 116.03, 116.27, 119.10, 121.06, 123.16, 123.25, 124.03, 126.26, 130.04, 145.77, 166.87.

Compound	M+H	M-H	Exact Mass	Observed Mass	% error
7Cl	262.0635	260.0479	261.0557	262.0629	0.000229

Compound **7I**:

^{1}H NMR (400 MHz, $CDCl_3$, δ in ppm): δ = 7.76 (d, 2H, *J* = 8.0 Hz, Ar-H), 7.50 (d, 1H, *J* = 8.0 Hz, Ar-H), 7.16 (t, 1H, *J* = 8.0 Hz, Ar-H), 7.01 (d, 2H, *J* = 8.0 Hz, Ar-H), 6.93 (d, 1H, *J* = 8.0 Hz, Ar-H), 3.82 (s, 2H, -NH_2), 2.44 (s, 3H, -CH_3).

^{13}C NMR (100 MHz, $CDCl_3$, δ in ppm): δ = 13.90, 89.82, 119.17, 121.08, 124.05, 124.07, 126.27, 129.89, 138.53, 145.78, 150.87, 166.37.

Compound	M+H	M-H	Exact Mass	Observed Mass	% error
7I	353.9991	351.9835	352.9913	353.9976	0.000424

Compound **6/F**:

^{1}H NMR (400 MHz, $CDCl_3$, δ in ppm): δ = 8.39 (s, 1H, -CH=N-), 8.19 (d, 2H, *J* = 8.0 Hz, Ar-H), 8.04 (d, 2H, *J* = 8.0 Hz, Ar-H), 7.98 (d, 1H, *J* = 8.0 Hz, Ar-H), 7.39-7.35 (m, 3H, Ar-H), 7.24-7.21 (m, 2H, Ar-H), 7.17-7.13 (m, 3H, Ar-H), 7.02 (d, 2H, *J* = 9.0 Hz, Ar-H), 4.08 (t, 2H, *J* = 6.6 Hz, -OCH_2-), 2.68 (s, 3H, -CH_3), 1.89-1.82 (m, 2H, -CH_2-), 1.55-1.48 (m, 2H, -CH_2-), 1.41-1.37 (m, 4H, -$(CH_2)_2$-), 0.95 (t, 3H, *J* = 7.0 Hz, -CH_3).

^{13}C NMR (100 MHz, $CDCl_3$, δ in ppm): δ = 14.07, 15.38, 22.62, 25.68, 29.07, 31.56, 68.39, 114.39, 116.05, 116.28, 122.30, 122.40, 123.16, 123.25, 126.41, 127.96, 129.81, 130.13, 132.40, 133.67, 134.51, 146.72, 152.47, 153.71, 159.40, 163.75, 164.64, 166.19.

FT-IR (cm^{-1}): HC=N stretching of an imine at 1608 cm^{-1}, C=O stretching band of ester at 1732 cm^{-1}, C-H stretching of alkanes at 2918 cm^{-1}

UV-vis (nm): 276 nm, 330 nm.

Compound	M+H	M-H	Exact Mass	Observed Mass	% error
6/F	554.2343	552.2187	553.2265	554.2361	0.000325

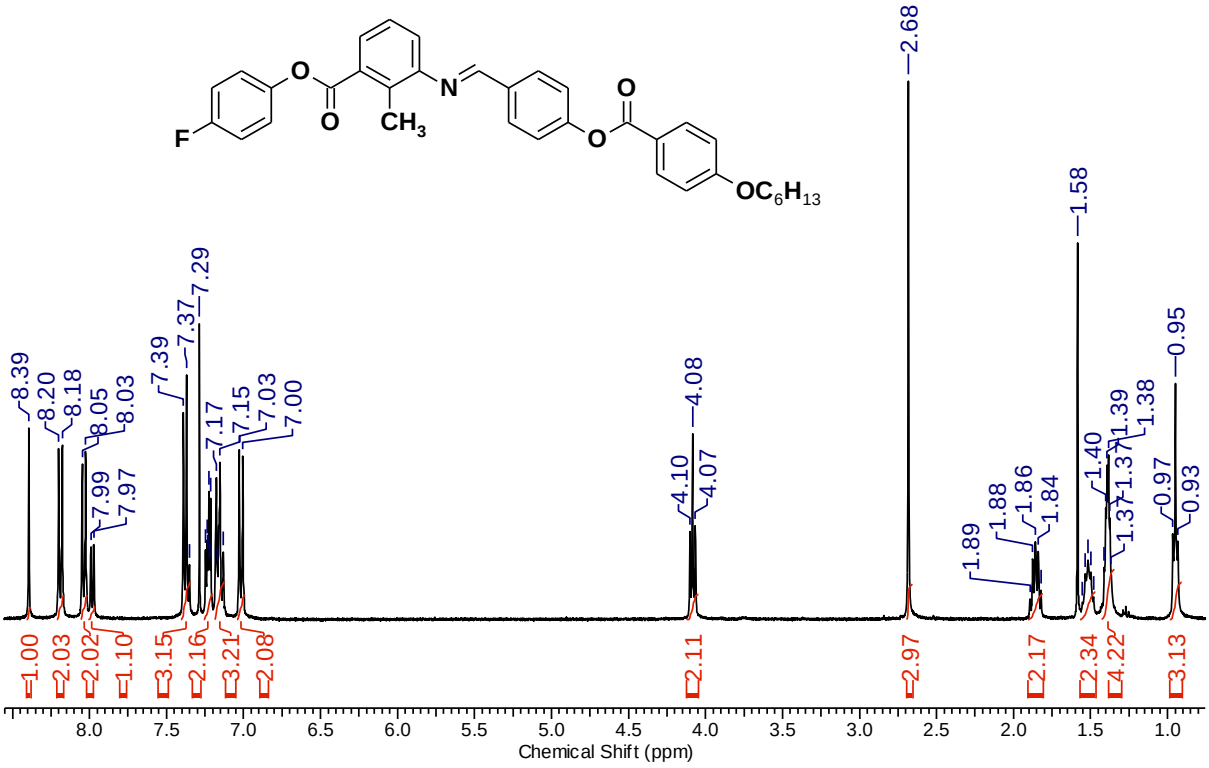

Figure S6: ^{1}H NMR of compound **6/F**.

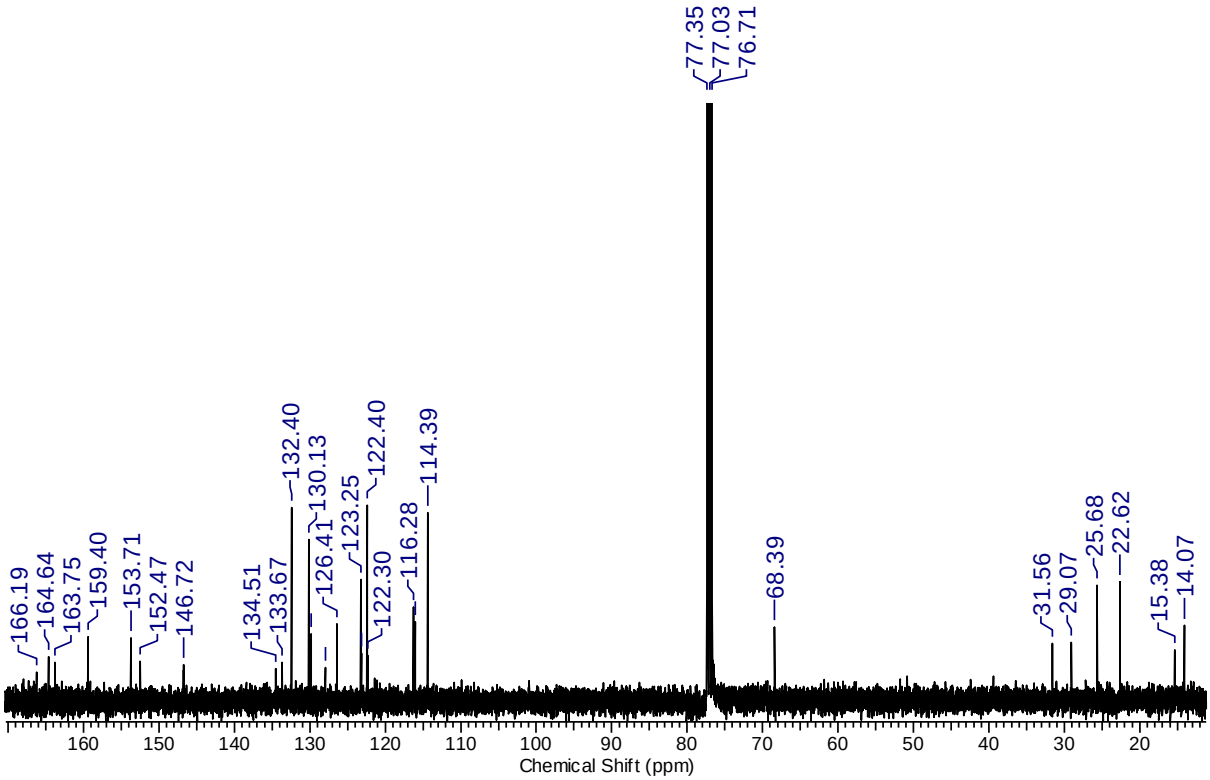

Figure S7: ^{13}C NMR of compound **6/F**.

Compound **6/Cl**:

^{1}H NMR (400 MHz, $CDCl_3$, δ in ppm): δ = 8.39 (s, 1H, -CH=N-), 8.19 (d, 2H, *J* = 8.0 Hz, Ar-H), 8.04 (d, 2H, *J* = 8.0 Hz, Ar-H), 7.98 (d, 1H, *J* = 8.0 Hz, Ar-H), 7.44 (d, 2H, *J* = 8.0 Hz, Ar-H), 7.39-7.35 (m, 3H, Ar-H), 7.22 (d, 2H, *J* = 8.0 Hz, Ar-H), 7.17 (d, 1H, *J* = 8.0 Hz, Ar-H), 7.02 (d, 2H, *J* = 8.0 Hz, Ar-H), 4.09 (t, 2H, *J* = 6.0 Hz, -OCH_2-), 2.68 (s, 3H, -CH_3), 1.89-1.82 (m, 2H, -CH_2-), 1.54-1.48 (m, 2H, -CH_2-), 1.40-1.39 (m, 4H, -$(CH_2)_2$-), 0.95 (t, 3H, *J* = 6.0 Hz, -CH_3).

^{13}C NMR (100 MHz, $CDCl_3$, δ in ppm): δ = 14.06, 15.37, 22.62, 25.68, 29.08, 31.57, 68.39, 114.39, 121.12, 122.36, 122.40, 123.21, 126.41, 127.98, 129.56, 129.69, 130.13, 131.25, 132.40, 133.66, 134.59, 149.41, 152.49, 153.72, 159.42, 163.75, 164.63, 165.88.

FT-IR (cm^{-1}): HC=N stretching of an imine at 1608 cm^{-1}, C=O stretching band of ester at 1732 cm^{-1}, C-H stretching of alkanes at 2922 cm^{-1}

UV-vis (nm): 276 nm, 330 nm.

Compound	**M+H**	**M-H**	**Exact Mass**	**Observed Mass**	**% error**
6/Cl	574.1796	572.1640	569.1969	574.1799	0.000052

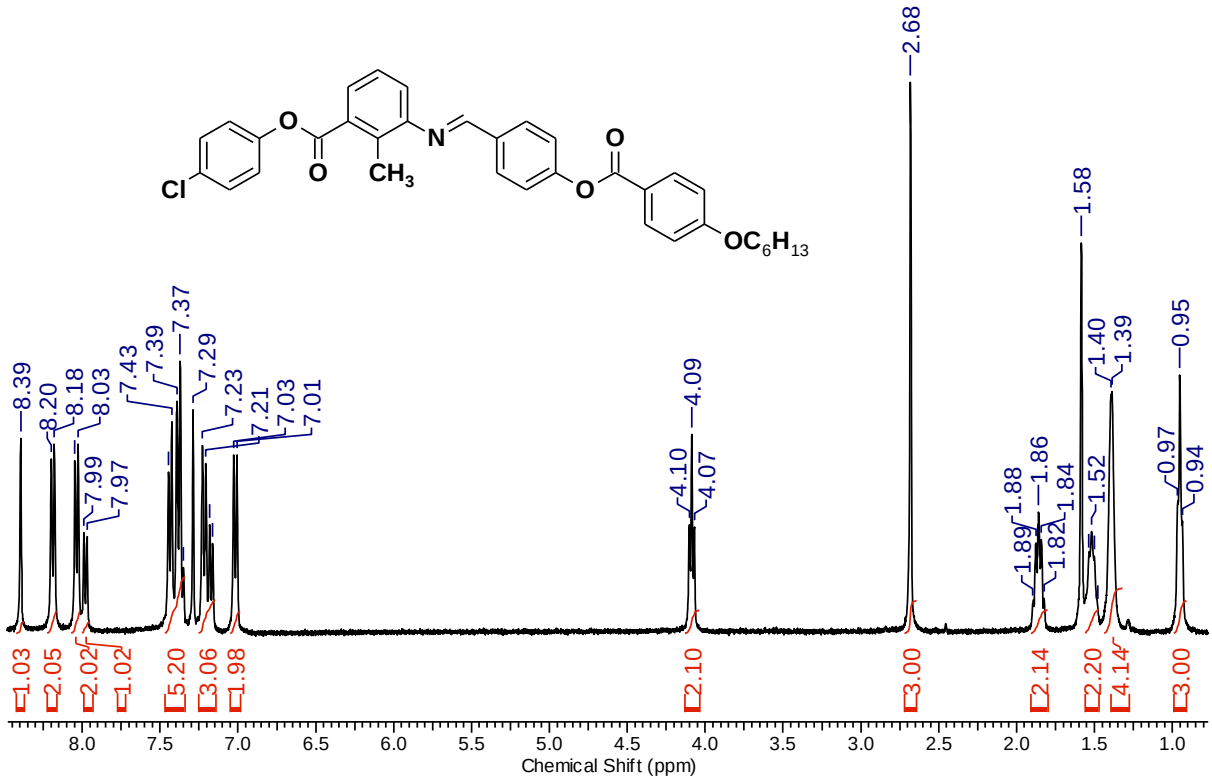

Figure S8: ^{1}H NMR of compound **6/Cl**.

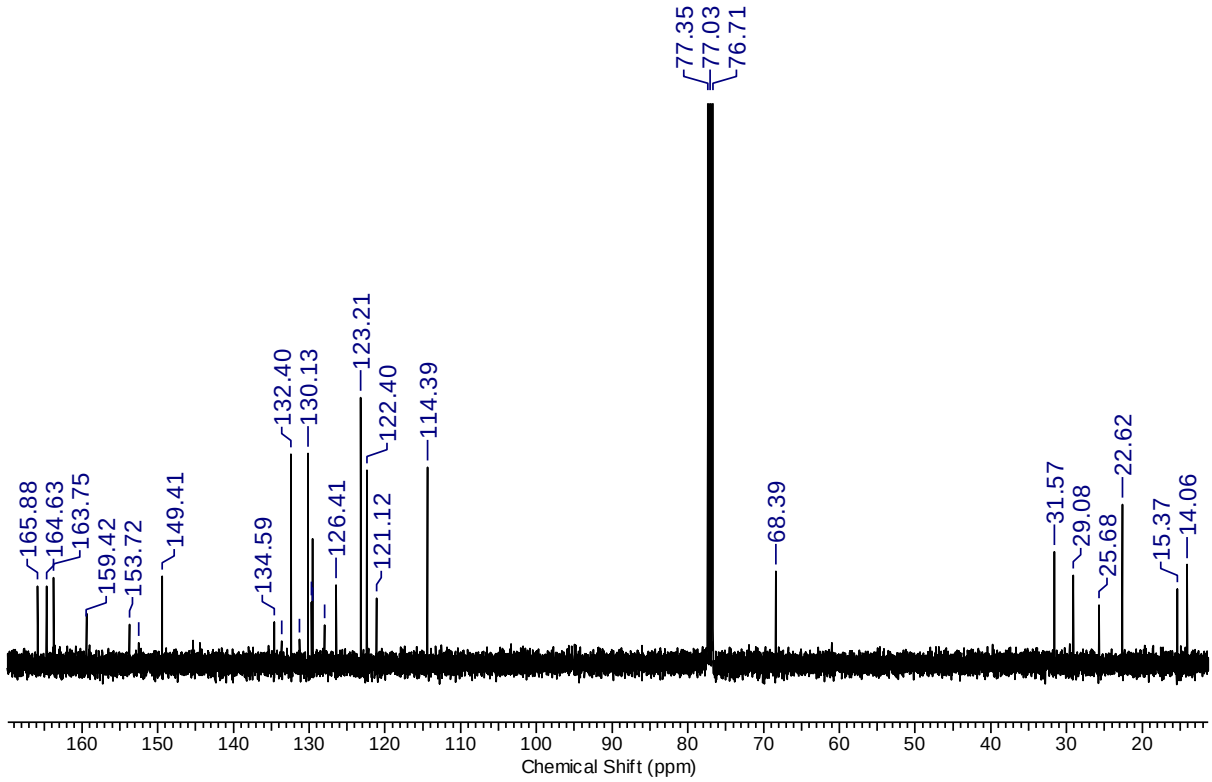

Figure S9: ^{13}C NMR of compound **6/Cl**.

Compound **6/Br**:

^{1}H NMR (400 MHz, $CDCl_3$, δ in ppm): δ = 8.39 (s, 1H, -CH=N-), 8.18 (d, 2H, *J* = 8.8 Hz, Ar-H), 8.03 (d, 2H, *J* = 8.0 Hz, Ar-H), 7.97 (d, 1H, *J* = 8.0 Hz, Ar-H), 7.58 (d, 2H, *J* = 8.0 Hz, Ar-H), 7.39-7.35 (m, 3H, Ar-H), 7.18-7.15 (m, 3H, Ar-H), 7.01 (d, 2H, *J* = 8.0 Hz, Ar-H), 4.08 (t, 2H, *J* = 6.4 Hz, $-OCH_2-$), 2.67 (s, 3H, $-CH_3$), 1.89-1.82 (m, 2H, $-CH_2-$), 1.54-1.49 (m, 2H, $-CH_2-$), 1.41-1.37 (m, 4H, $-(CH_2)_2-$), 0.95 (t, 3H, *J* = 6.0 Hz, $-CH_3$).

^{13}C NMR (100 MHz, $CDCl_3$, δ in ppm): δ = 14.07, 15.38, 22.62, 25.68, 29.07, 31.57, 68.39, 114.39, 118.96, 121.11, 122.38, 122.41, 123.64, 126.42, 127.99, 129.66, 130.14, 132.40, 132.55, 133.65, 134.59, 149.96, 152.49, 153.72, 159.43, 163.75, 164.64, 165.79.

FT-IR (cm^{-1}): HC=N stretching of an imine at 1606 cm^{-1}, C=O stretching band of ester at 1732 cm^{-1}, C-H stretching of alkanes at 2922 cm^{-1}

UV-vis (nm): 276 nm, 330 nm.

Compound	M+H	M-H	Exact Mass	Observed Mass	% error
6/Br	614.1542	612.1386	613.1464	614.1561	0.000309

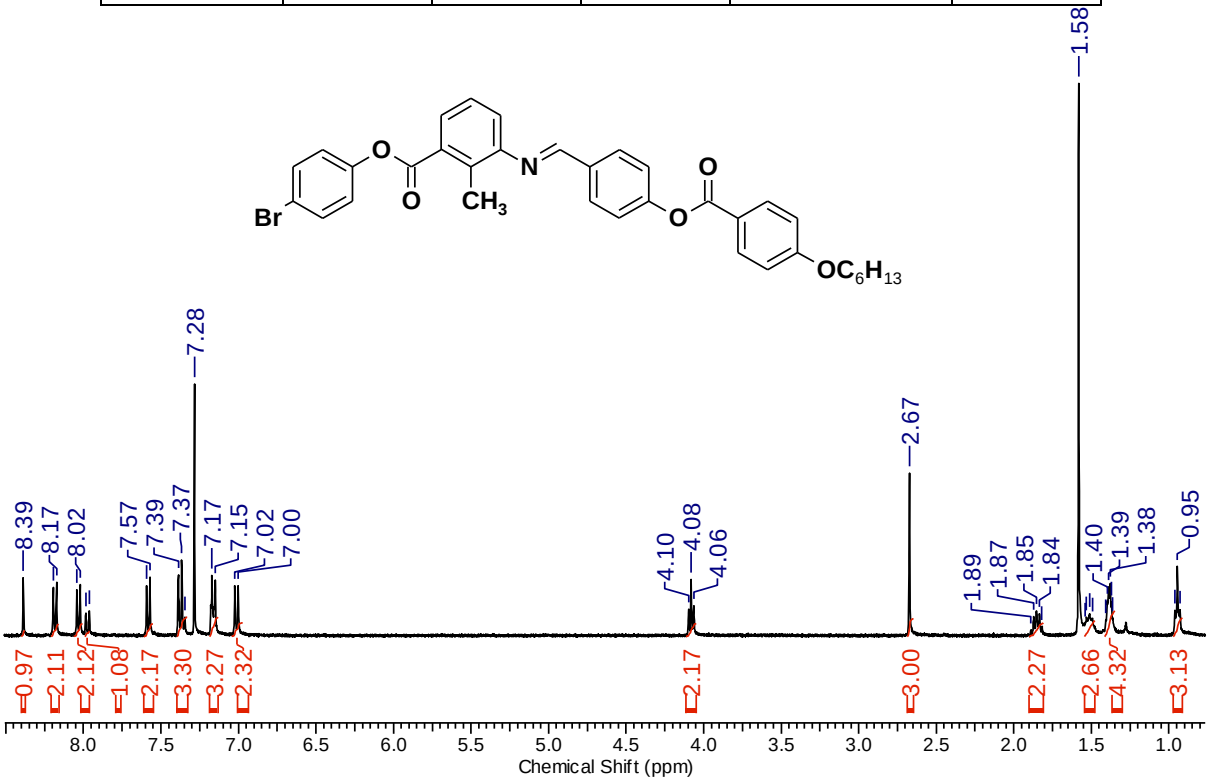

Figure S10: ^{1}H NMR of compound **6/Br**.

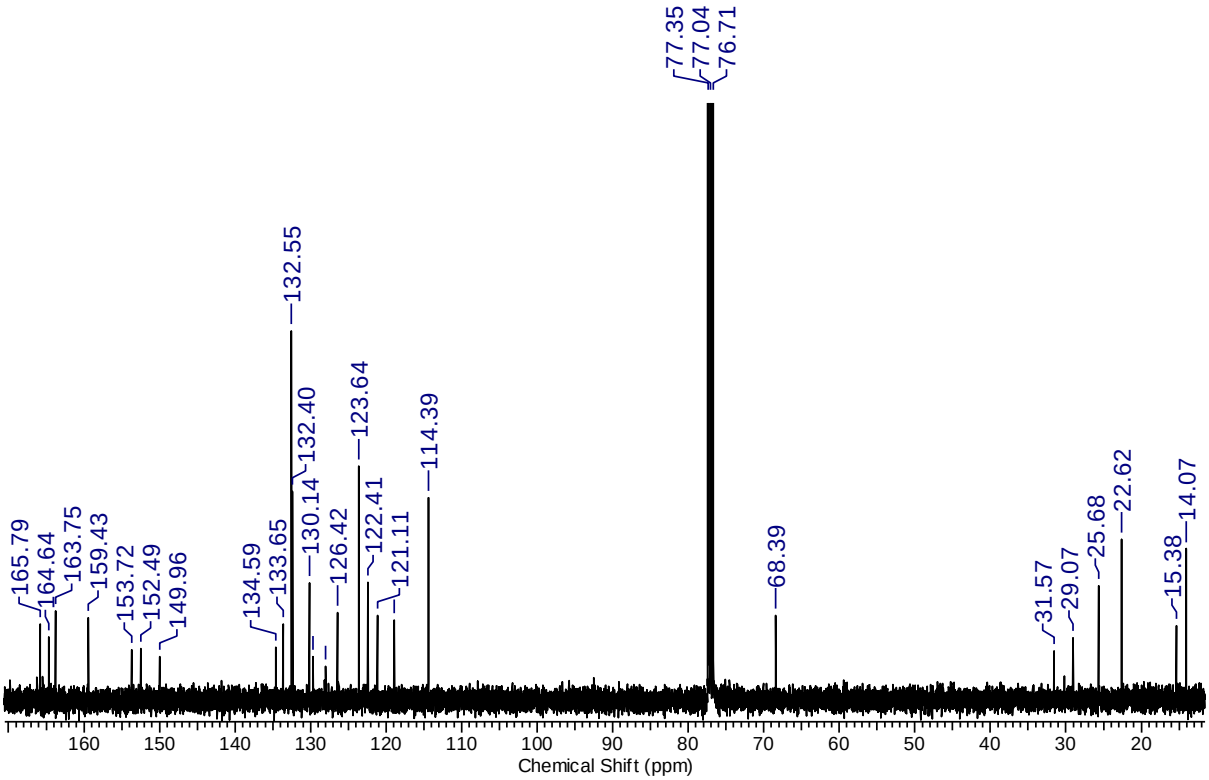

Figure S11: ^{13}C NMR of compound **6/Br**.

Compound **6/I**:

^{1}H NMR (400 MHz, $CDCl_3$, δ in ppm): δ = 8.39 (s, 1H, -CH=N-), 8.19 (d, 2H, J = 8.8 Hz, Ar-H), 8.03 (d, 2H, J = 8.0 Hz, Ar-H), 7.97 (d, 1H, J = 8.0 Hz, Ar-H), 7.77 (d, 2H, J = 8.0 Hz, Ar-H), 7.39-7.34 (m, 3H, Ar-H), 7.17 (d, 1H, J = 4.0 Hz, Ar-H), 7.05-7.00 (m, 4H, Ar-H), 4.08 (t, 2H, J = 6.4 Hz, -OCH_2-), 2.67 (s, 3H, -CH_3), 1.88-1.82 (m, 2H, -CH_2-), 1.55-1.48 (m, 2H, -CH_2-), 1.41-1.37 (m, 4H, -$(CH_2)_2$-), 0.95 (t, 3H, J = 6.0 Hz, -CH_3).

^{13}C NMR (100 MHz, $CDCl_3$, δ in ppm): δ = 14.07, 15.37, 22.62, 25.68, 29.07, 31.56, 68.39, 89.88, 114.39, 121.11, 122.38, 122.40, 124.05, 126.41, 127.98, 129.67, 130.13, 132.40, 133.65, 134.59, 138.55, 145.52, 150.80, 152.49, 153.72, 159.43, 164.64, 165.75.

FT-IR (cm^{-1}): HC=N stretching of an imine at 1605 cm^{-1}, C=O stretching band of ester at 1732 cm^{-1}, C-H stretching of alkanes at 2922 cm^{-1}

UV-vis (nm): 276 nm, 330 nm.

Compound	**M+H**	**M-H**	**Exact Mass**	**Observed Mass**	**% error**
6/I	662.1403	660.1247	661.1325	662.1404	0.000015

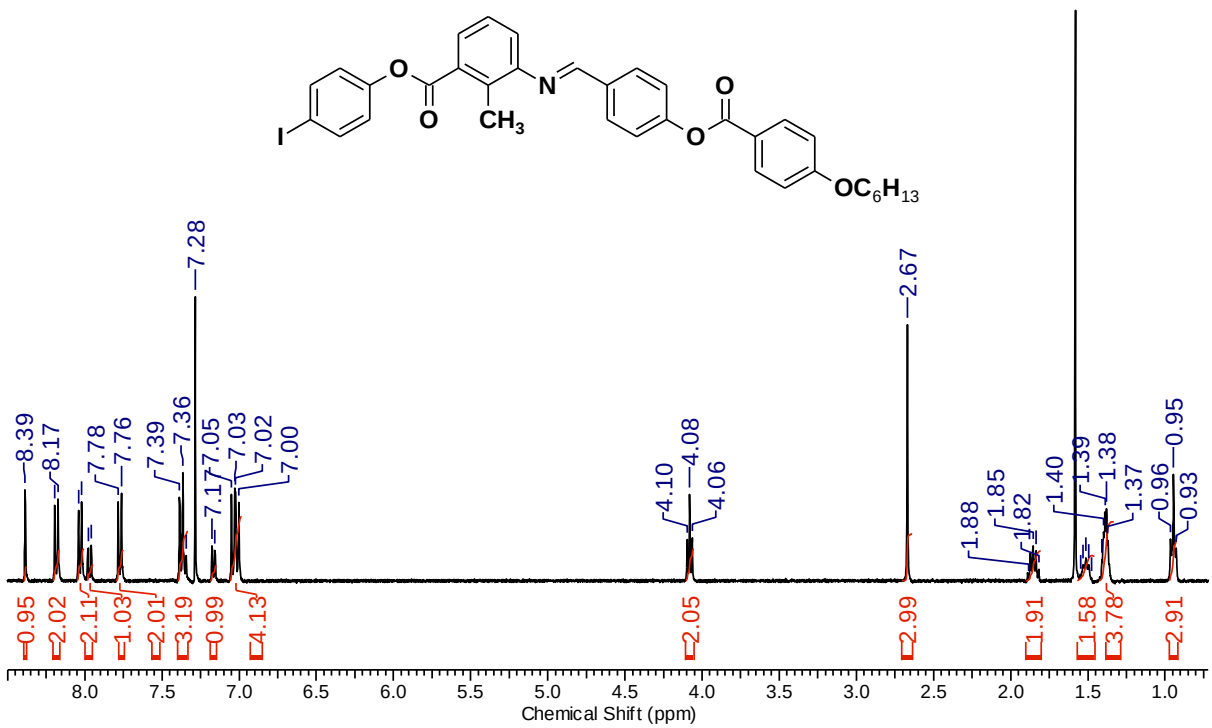

Figure S12: ^{1}H NMR of compound **6/I**.

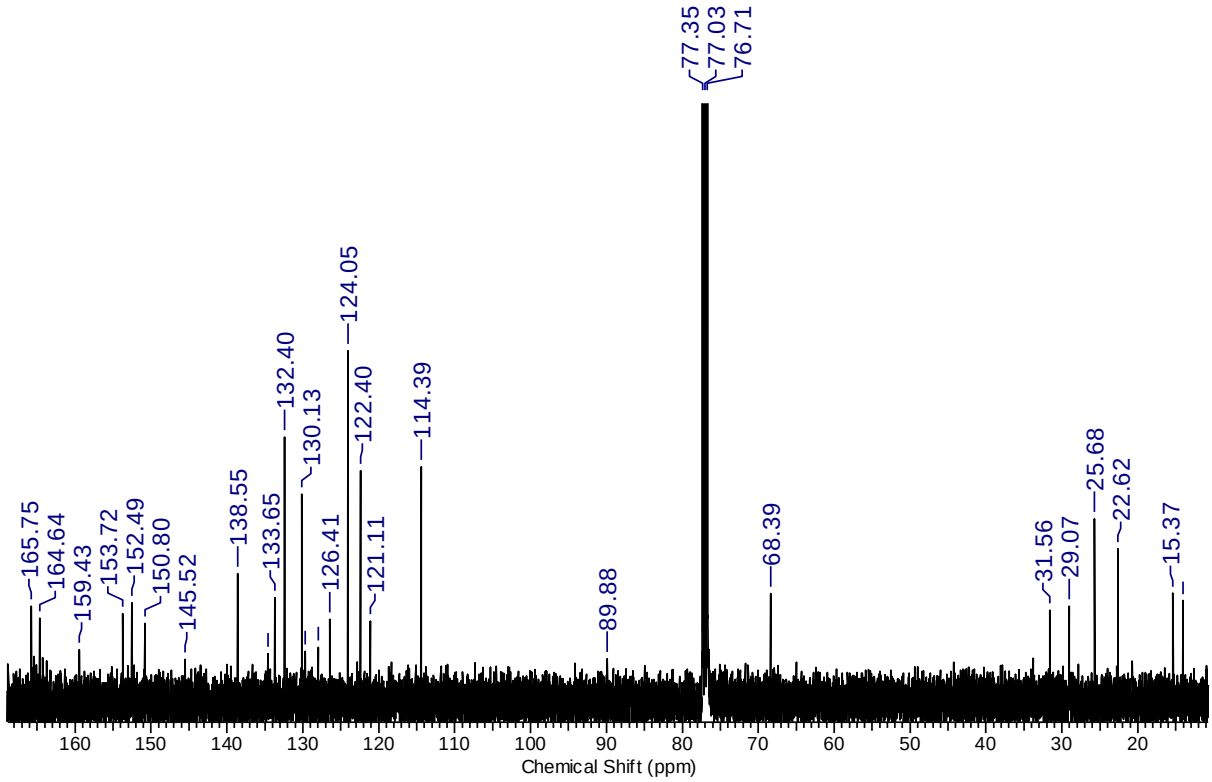

Figure S13: ^{13}C NMR of compound **6/I**.

Compound **8/F**:

^{1}H NMR (400 MHz, $CDCl_3$, δ in ppm): δ = 8.39 (s, 1H, -CH=N-), 8.19 (d, 2H, *J* = 8.0 Hz, Ar-H), 8.04 (d, 2H, *J* = 8.0 Hz, Ar-H), 7.98 (d, 1H, *J* = 8.0 Hz, Ar-H), 7.39-7.35 (m, 3H, Ar-H), 7.23-7.21 (m, 2H, Ar-H), 7.18-7.13 (m, 3H, Ar-H), 7.01 (d, 2H, *J* = 8.8 Hz, Ar-H), 4.08 (t, 2H, *J* = 6.5 Hz, $-OCH_2-$), 2.68 (s, 3H, $-CH_3$), 1.89-1.82 (m, 2H, $-CH_2-$), 1.55-1.47 (m, 2H, $-CH_2-$), 1.37-1.28 (m, 8H, $-(CH_2)_4-$), 0.92 (t, 3H, *J* = 6.0 Hz, $-CH_3$).

^{13}C NMR (100 MHz, $CDCl_3$, δ in ppm): δ = 14.14, 15.38, 22.68, 26.01, 29.11, 29.25, 29.35, 31.83, 68.39, 114.39, 116.05, 116.29, 121.11, 122.30, 122.40, 123.17, 123.25, 126.41, 127.96, 129.80, 130.13, 132.40, 133.67, 134.51, 152.47, 153.71, 159.40, 163.75, 164.64, 166.19.

FT-IR (cm^{-1}): HC=N stretching of an imine at 1609 cm^{-1}, C=O stretching band of ester at 1731 cm^{-1}, C-H stretching of alkanes at 2919 cm^{-1}

UV-vis (nm): 276 nm, 330 nm.

Compound	M+H	M-H	Exact Mass	Observed Mass	% error
8/F	582.2656	580.2500	581.2578	582.2678	0.000378

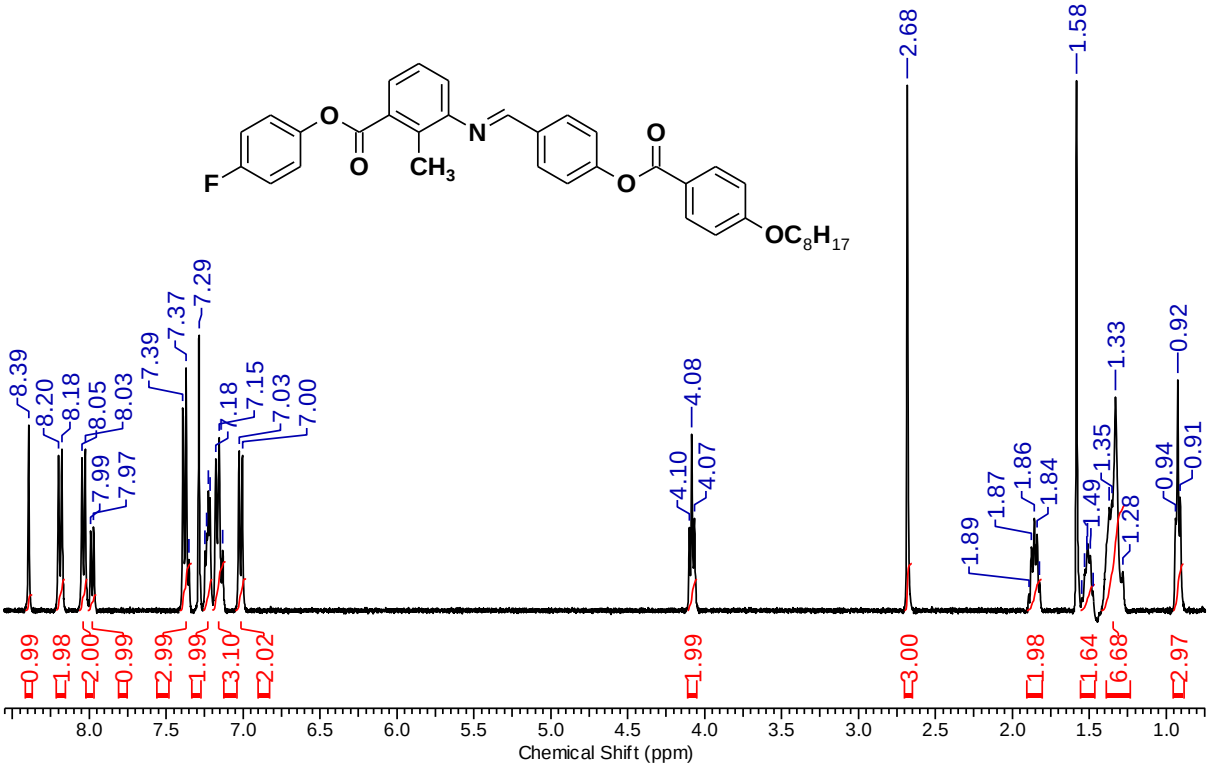

Figure S14: ^{1}H NMR of compound **8/F**.

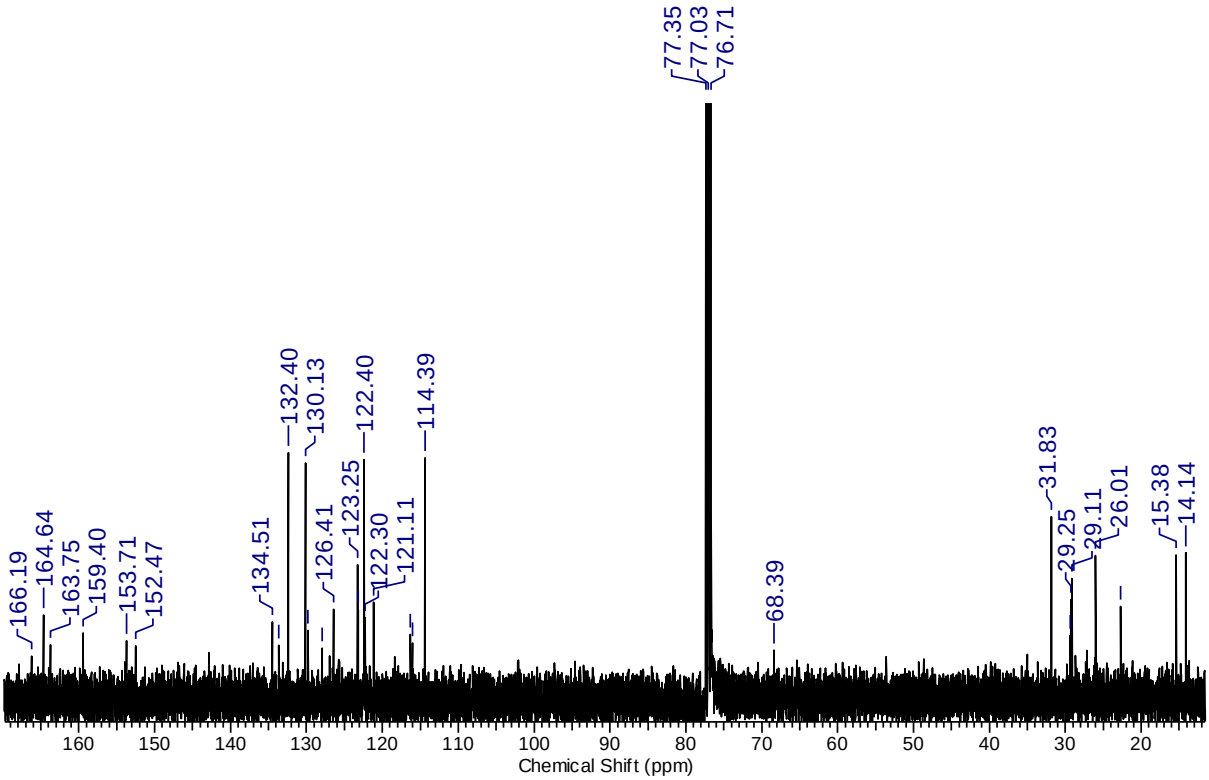

Figure S15: ^{13}C NMR of compound **8/F**.

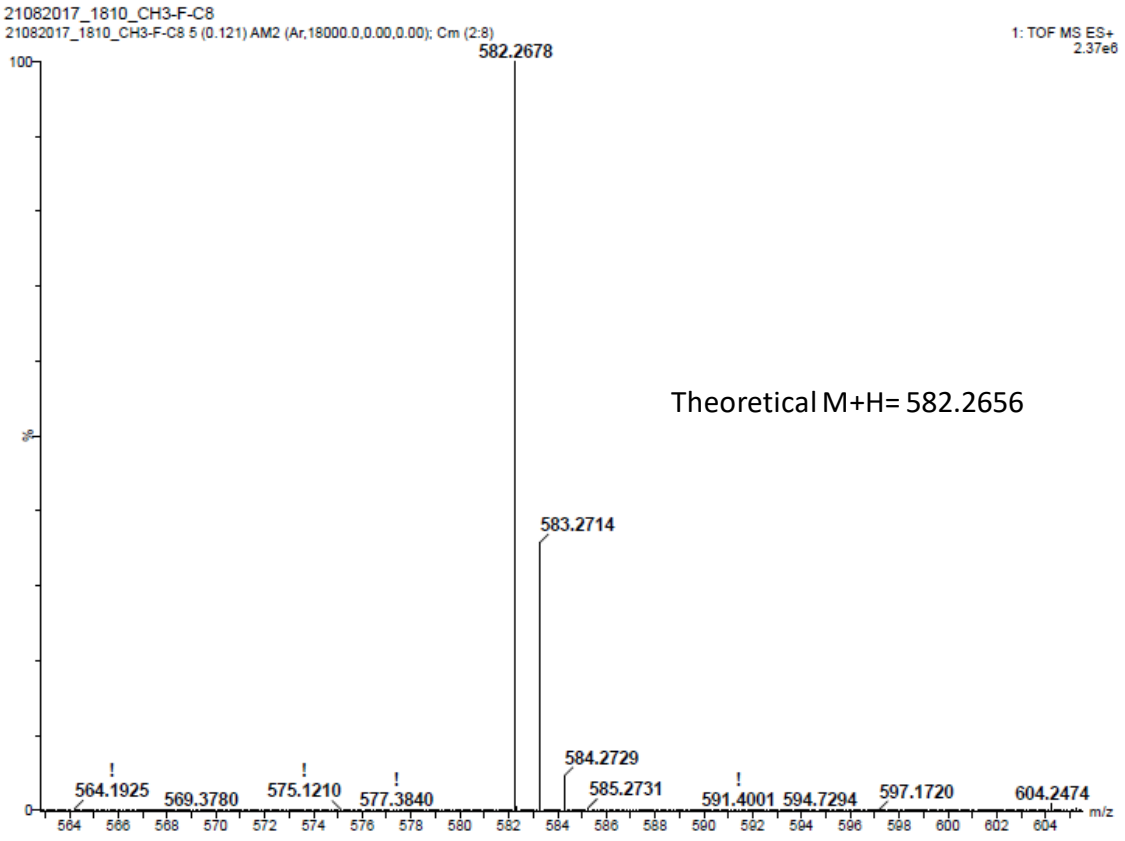

Figure S16: ESI spectrum of compound **8/F**.

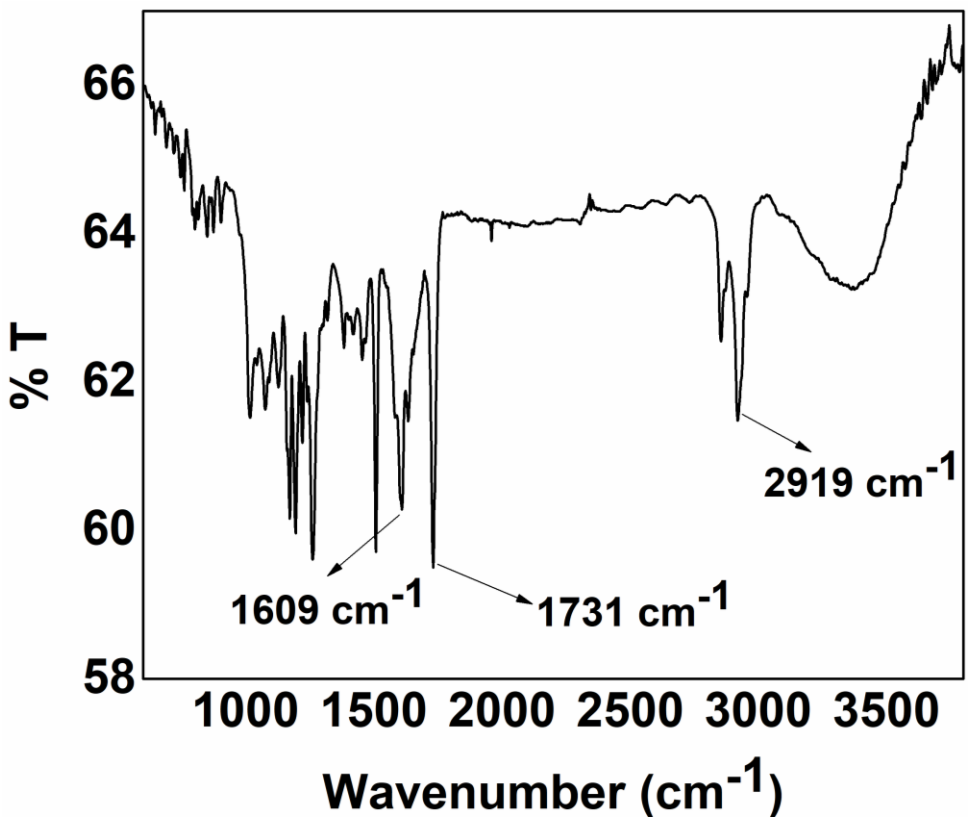

Figure S17: FT-IR spectrum of compound **8/F**.

Compound **8/Cl**:

^{1}H NMR (400 MHz, $CDCl_3$, δ in ppm): δ = 8.39 (s, 1H, -CH=N-), 8.19 (d, 2H, *J* = 8.0 Hz, Ar-H), 8.03 (d, 2H, *J* = 8.0 Hz, Ar-H), 7.98 (d, 1H, *J* = 8.0 Hz, Ar-H), 7.43 (d, 2H, *J* = 8.0 Hz, Ar-H), 7.39-7.35 (m, 3H, Ar-H), 7.22 (d, 2H, *J* = 8.6 Hz, Ar-H), 7.17 (d, 1H, *J* = 8.0 Hz, Ar-H), 7.01 (d, 2H, *J* = 9.0 Hz, Ar-H), 4.08 (t, 2H, *J* = 6.5 Hz, -OCH_2-), 2.68 (s, 3H, -CH_3), 1.89-1.82 (m, 2H, -CH_2-), 1.55-1.47 (m, 2H, -CH_2-), 1.42-1.33 (m, 8H, -$(CH_2)_4$-), 0.92 (t, 3H, *J* = 6.0 Hz, -CH_3).

^{13}C NMR (100 MHz, $CDCl_3$, δ in ppm): δ = 14.14, 15.38, 22.68, 26.01, 29.11, 29.25, 29.35, 31.83, 68.39, 114.39, 121.11, 122.37, 122.41, 123.21, 126.42, 127.98, 129.56, 129.58, 130.13, 131.57, 132.40, 133.65, 134.59, 149.40, 152.49, 153.72, 159.43, 163.75, 164.64, 165.89.

FT-IR (cm^{-1}): HC=N stretching of an imine at 1607 cm^{-1}, C=O stretching band of ester at 1731 cm^{-1}, C-H stretching of alkanes at 2922 cm^{-1}

UV-vis (nm): 276 nm, 330 nm.

Compound	M+H	M-H	Exact Mass	Observed Mass	% error
8/Cl	598.2360	596.2204	597.2282	598.2389	0.000485

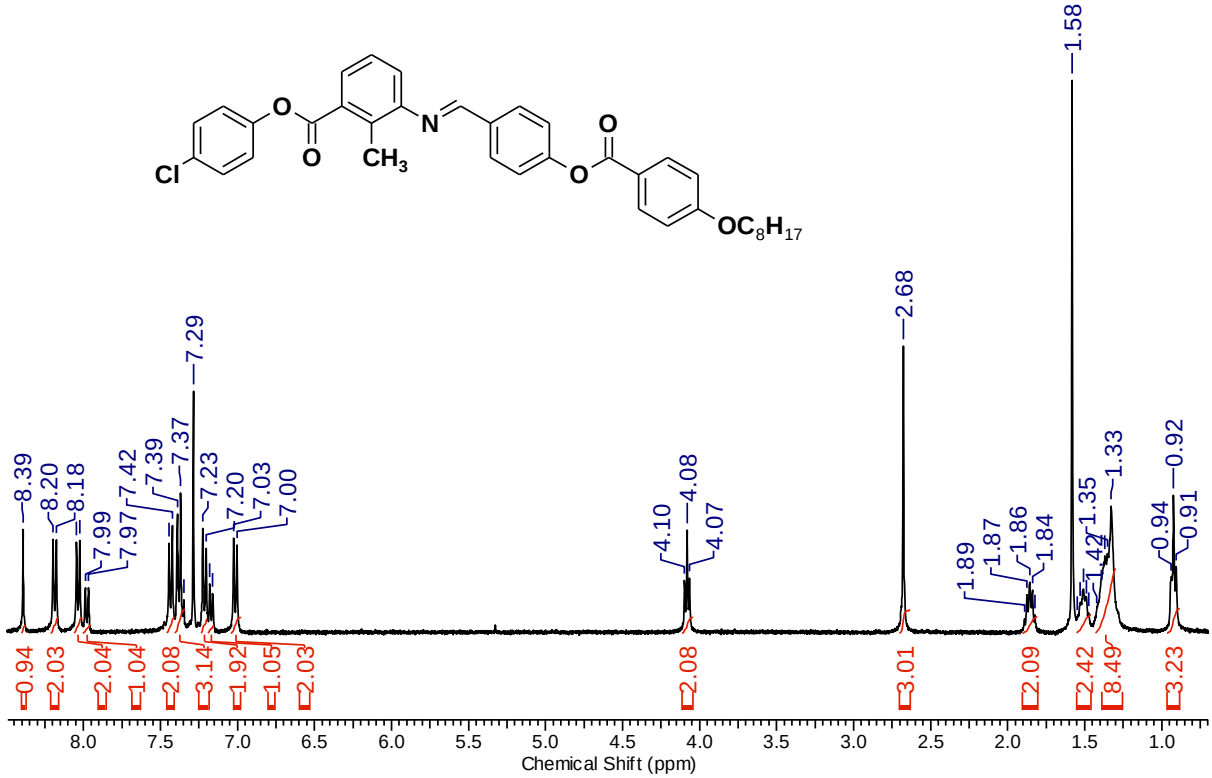

Figure S18: ^{1}H NMR of compound **8/Cl**.

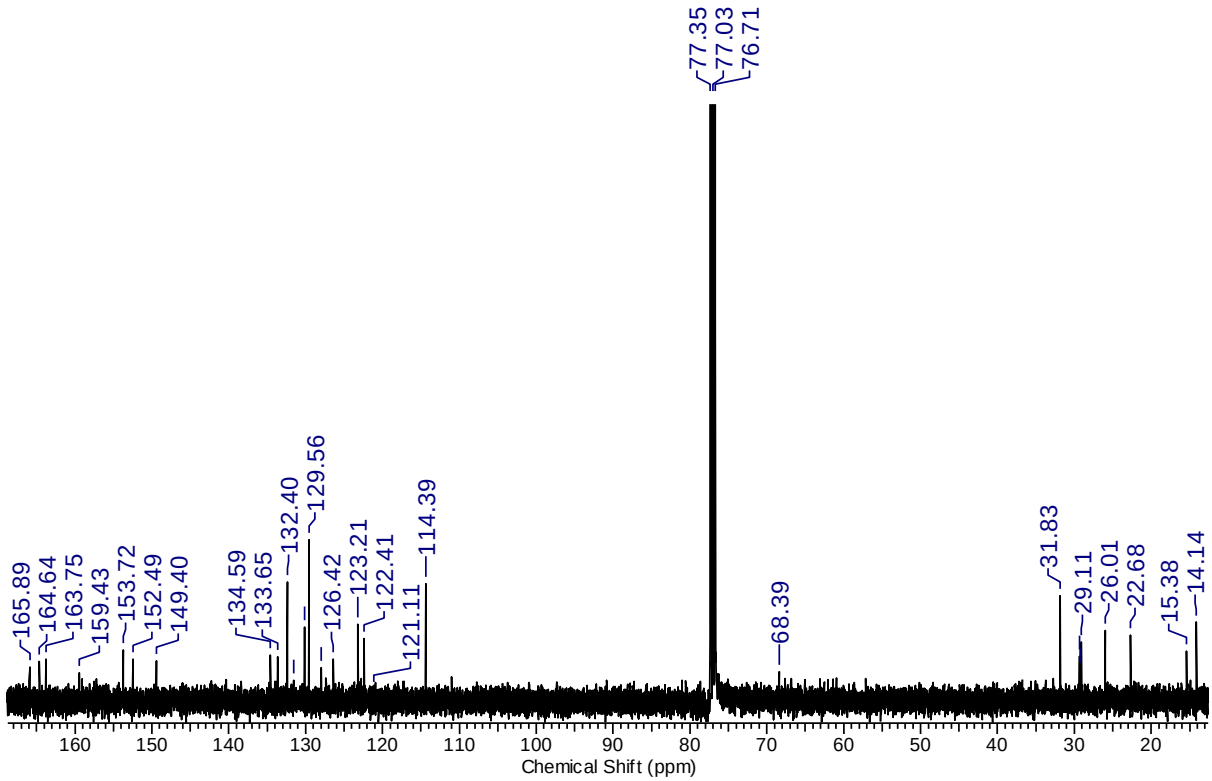

Figure S19: ^{13}C NMR of compound **8/Cl**.

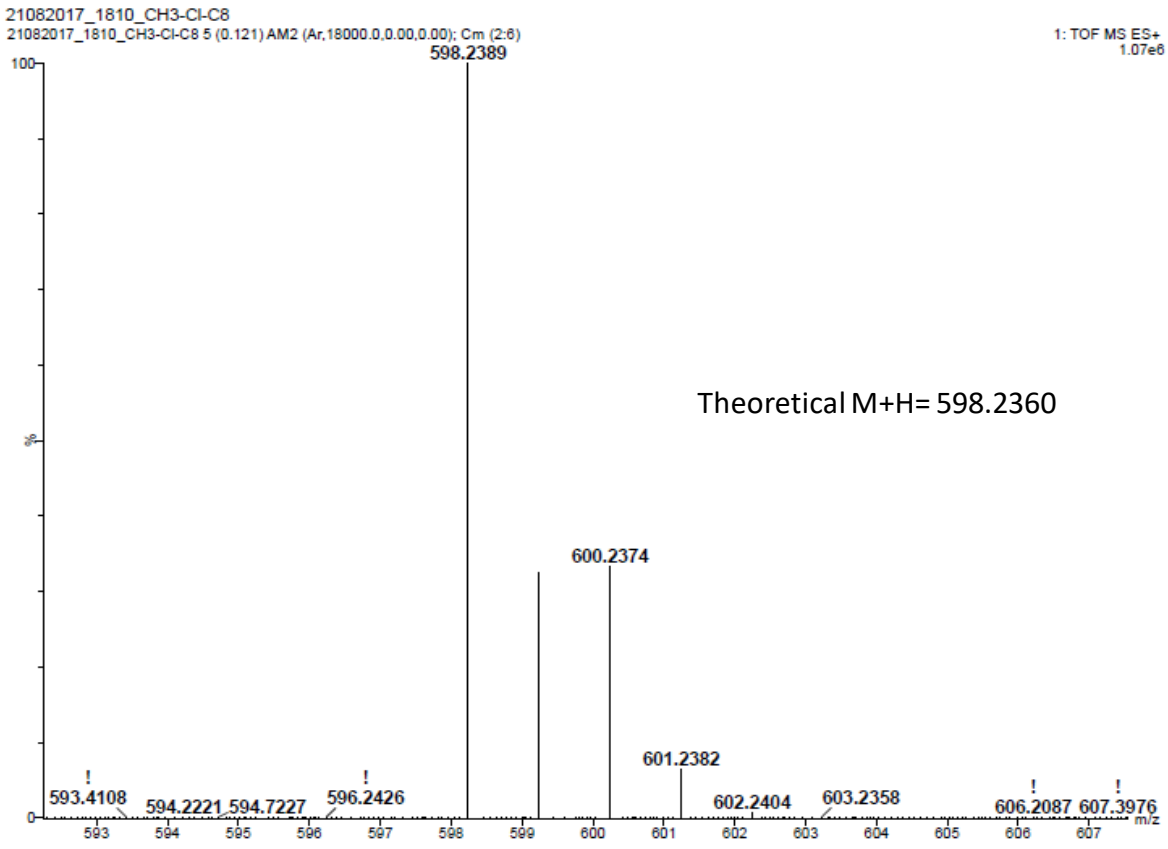

Figure S20: ESI spectrum of compound **8/Cl**.

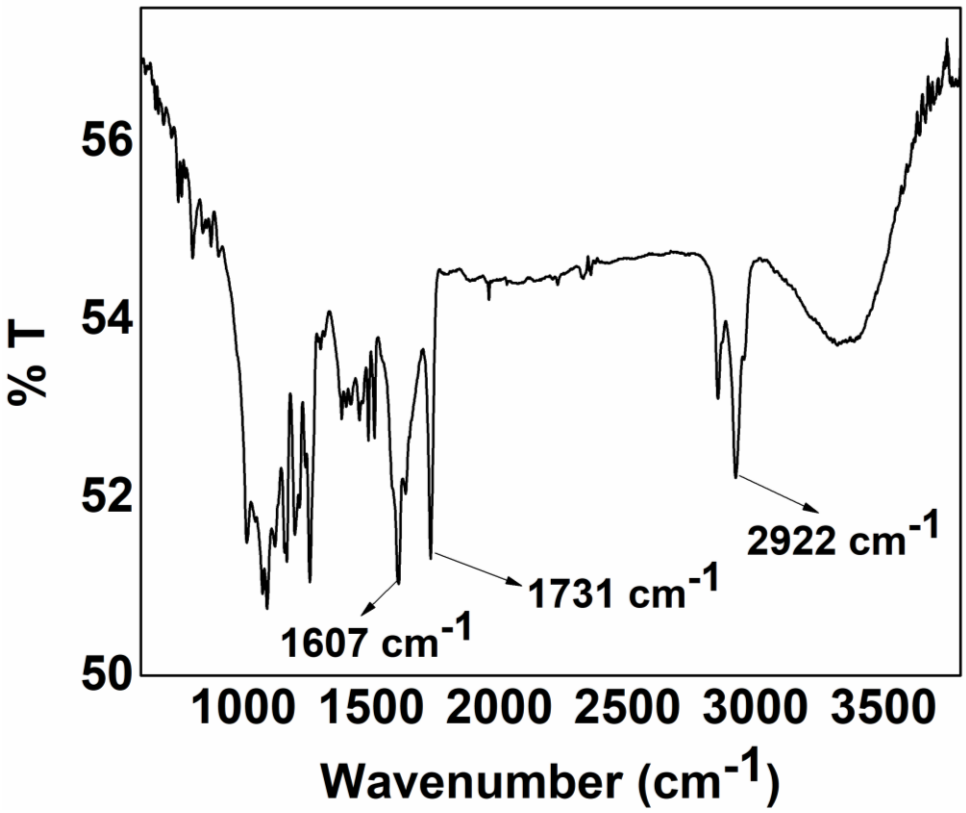

Figure S21: FT-IR spectrum of compound **8/Cl**.

Compound **8/I**:

^{1}H NMR (400 MHz, $CDCl_3$, δ in ppm): δ = 8.39 (s, 1H, -CH=N-), 8.19 (dd, 2H, *J* = 4.0, 8.0 Hz, Ar-H), 8.03 (dd, 2H, *J* = 1.8, 6.7 Hz, Ar-H), 7.97 (dd, 1H, *J* = 1.2, 8.0 Hz, Ar-H), 7.78 (dd, 2H, *J* = 4.0, 8.0 Hz, Ar-H), 7.39-7.35 (m, 3H, Ar-H), 7.17 (dd, 1H, *J* = 1.0, 7.8 Hz, Ar-H), 7.05-7.00 (m, 4H, Ar-H), 4.08 (t, 2H, *J* = 6.0 Hz, $-OCH_2-$), 2.67 (s, 3H, $-CH_3$), 1.89-1.82 (m, 2H, $-CH_2-$), 1.54-1.47 (m, 2H, $-CH_2-$), 1.42-1.31 (m, 8H, $-(CH_2)_4-$), 0.92 (t, 3H, *J* = 8.0 Hz, $-CH_3$).

^{13}C NMR (100 MHz, $CDCl_3$, δ in ppm): δ = 14.13, 15.38, 22.68, 25.99, 29.11, 29.24, 29.34, 31.82, 68.39, 89.87, 114.39, 121.11, 122.40, 124.05, 126.42, 127.98, 129.68, 130.13, 132.40, 133.65, 134.61, 138.55, 150.80, 152.49, 153.72, 159.42, 163.75, 164.64, 165.73, 167.73.

FT-IR (cm^{-1}): HC=N stretching of an imine at 1603 cm^{-1}, C=O stretching band of ester at 1731 cm^{-1}, C-H stretching of alkanes at 2923 cm^{-1}

UV-vis (nm): 276 nm, 330 nm.

Compound	**M+H**	**M-H**	**Exact Mass**	**Observed Mass**	**% error**
8/I	690.1716	688.1560	689.1638	690.1691	0.000362

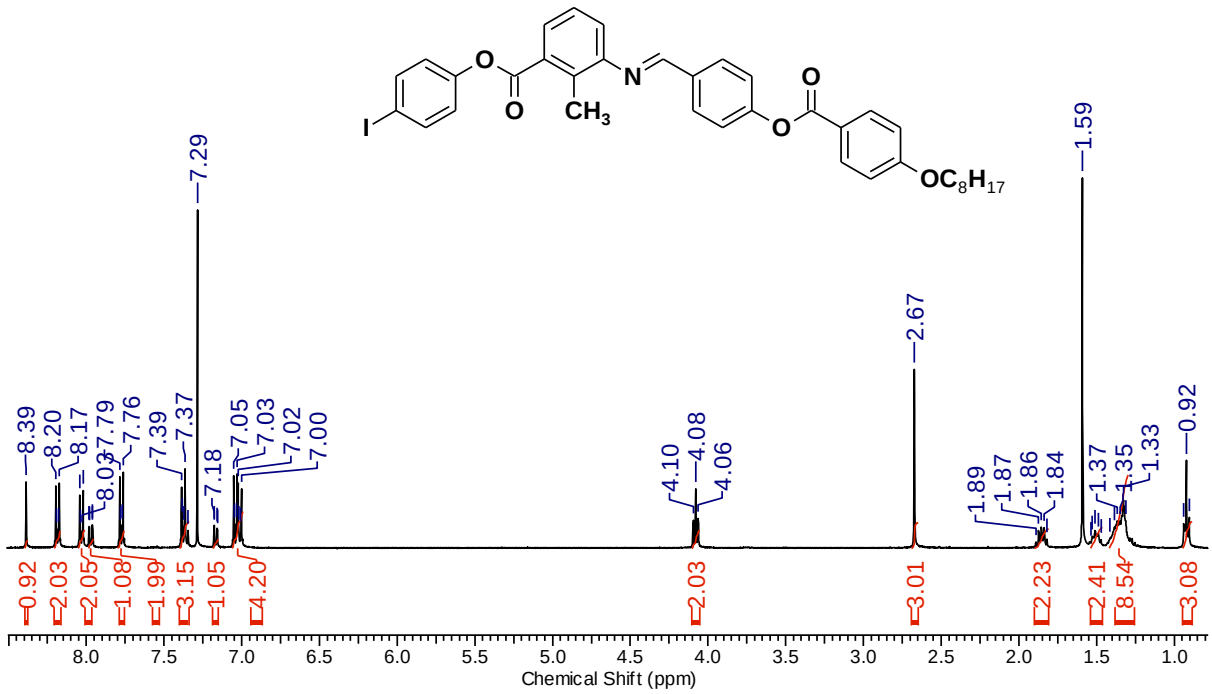

Figure S22: ^{1}H NMR of compound **8/I**.

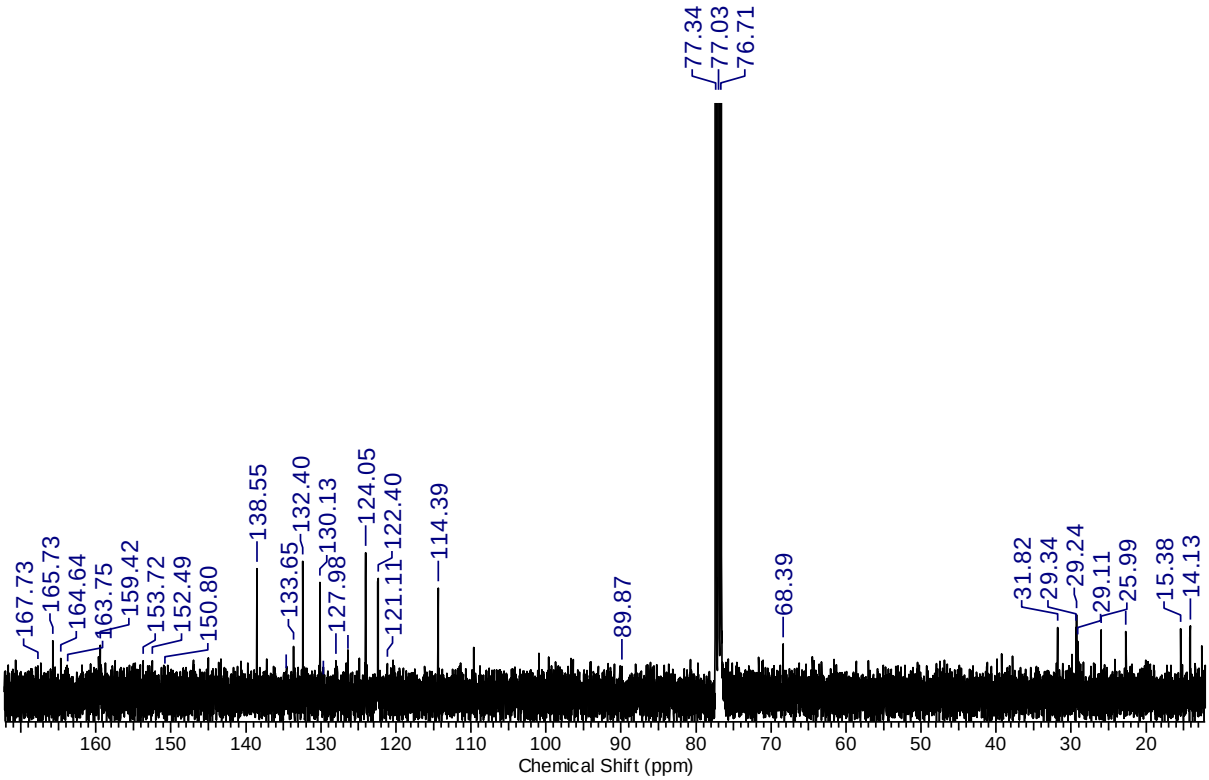

Figure S23: ^{13}C NMR of compound **8/I**.

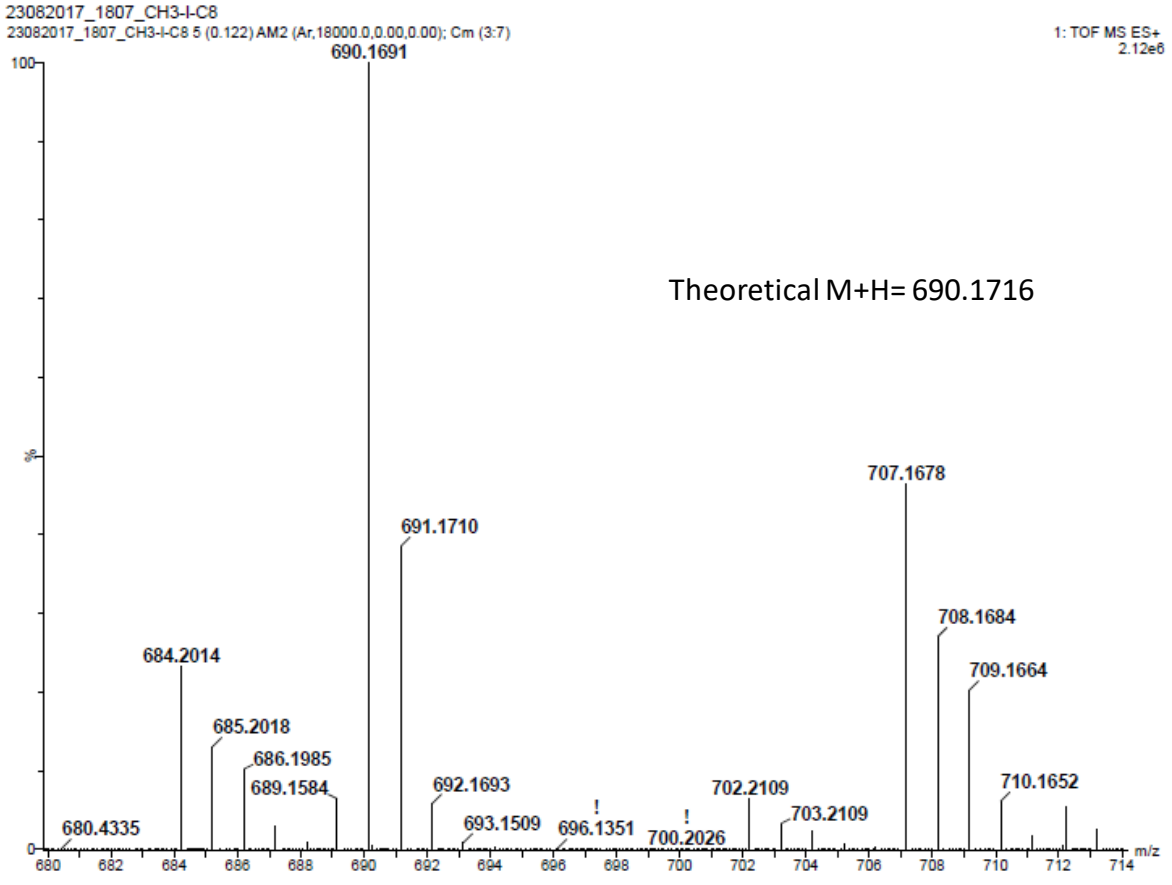

Figure S24: ESI spectrum of compound **8/I**.

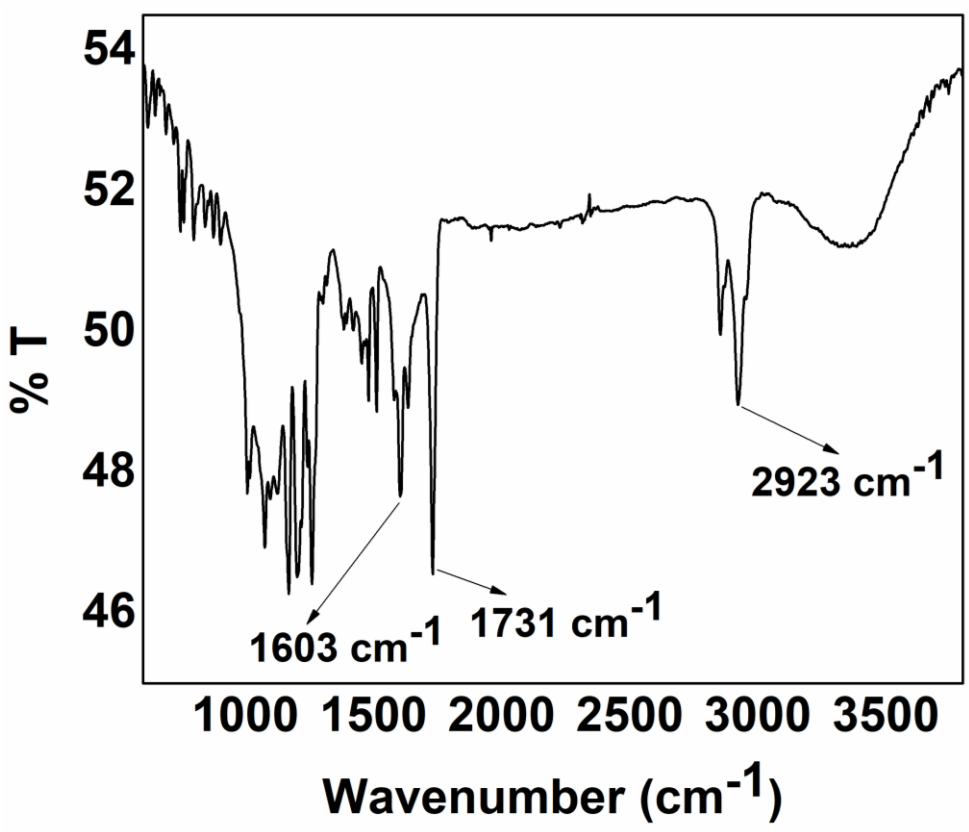

Figure S25: FT-IR spectrum of compound **8/I**.

Compound **10/F**:

^{1}H NMR (400 MHz, $CDCl_3$, δ in ppm): δ = 8.39 (s, 1H, -CH=N-), 8.19 (dd, 2H, *J* = 4.0, 8.0 Hz, Ar-H), 8.03 (dd, 2H, *J* = 2.0, 6.8 Hz, Ar-H), 7.98 (dd, 1H, *J* = 1.2, 7.8 Hz, Ar-H), 7.39-7.35 (m, 3H, Ar-H), 7.25-7.21 (m, 2H, Ar-H), 7.18-7.13 (m, 3H, Ar-H), 7.02 (dd, 2H, *J* = 2.1, 7.0 Hz, Ar-H), 4.08 (t, 2H, *J* = 6.0 Hz, -OCH_2-), 2.68 (s, 3H, -CH_3), 1.89-1.82 (m, 2H, -CH_2-), 1.53-1.47 (m, 2H, -CH_2-), 1.39-1.31 (m, 12H, -$(CH_2)_6$-), 0.91 (t, 3H, *J* = 6.0 Hz, -CH_3).

^{13}C NMR (100 MHz, $CDCl_3$, δ in ppm): δ = 14.16, 15.38, 22.72, 26.00, 29.11, 29.35, 29.39, 29.58, 31.93, 68.40, 114.40, 116.06, 116.29, 121.13, 122.31, 122.42, 123.18, 123.26, 126.42, 127.97, 130.15, 132.41, 133.68, 134.53, 146.73, 146.76, 152.49, 153.73, 159.10, 159.42, 163.77, 166.21.

FT-IR (cm^{-1}): HC=N stretching of an imine at 1607 cm^{-1}, C=O stretching band of ester at 1733 cm^{-1}, C-H stretching of alkanes at 2918 cm^{-1}

UV-vis (nm): 276 nm, 330 nm.

Compound	**M+H**	**M-H**	**Exact Mass**	**Observed Mass**	**% error**
10/F	610.2969	608.2813	609.2891	610.2939	0.000492

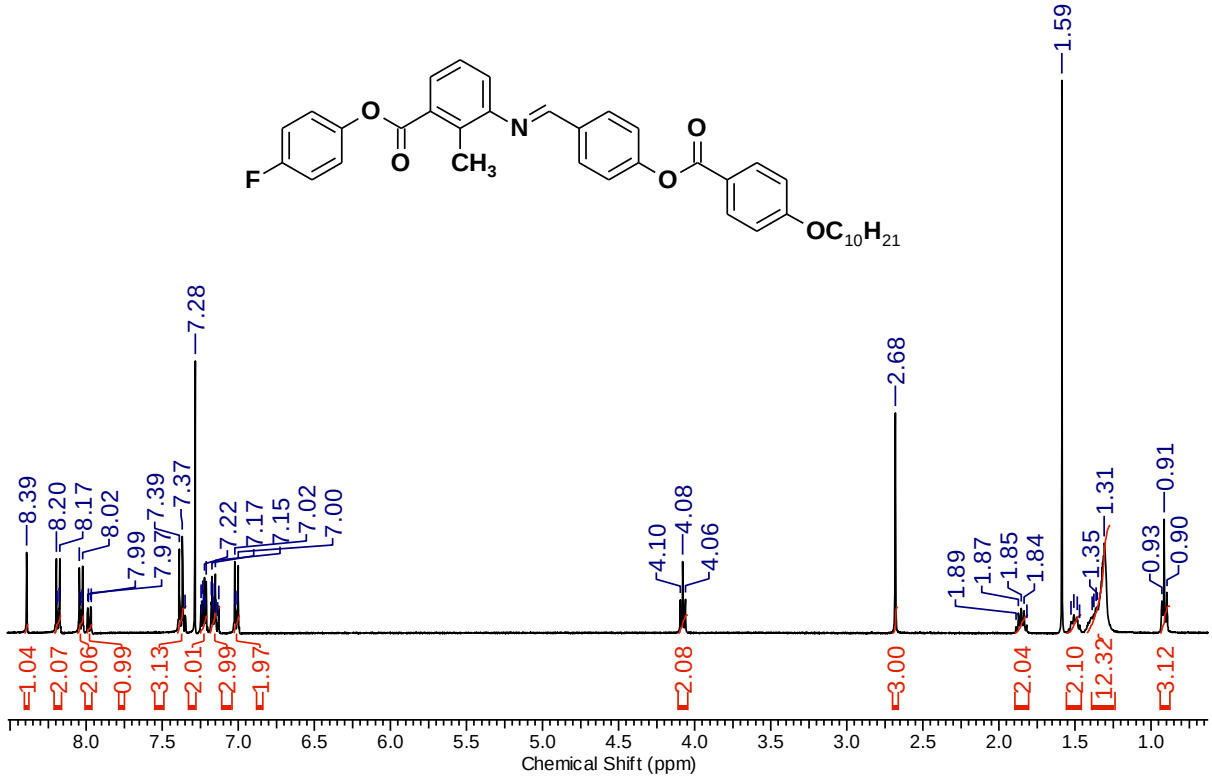

Figure S26: ^{1}H NMR of compound **10/F**.

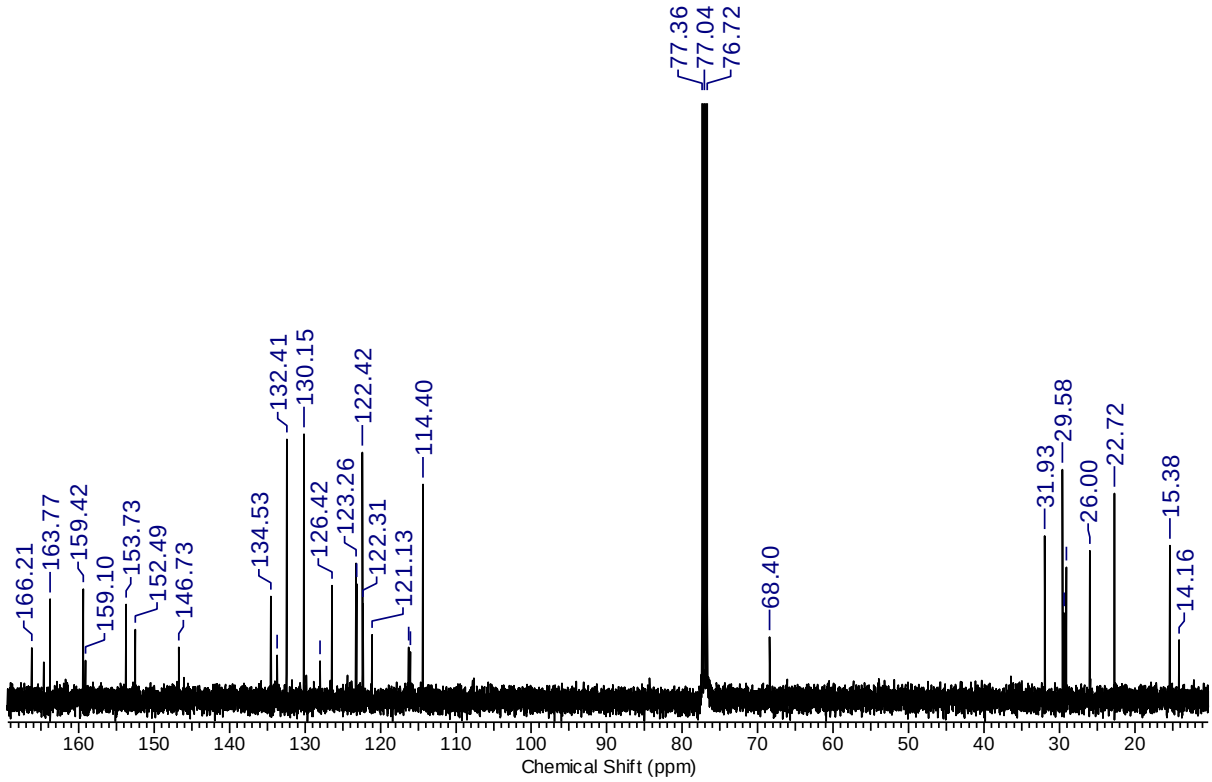

Figure S27: ^{13}C NMR of compound **10/F**.

Compound **10/Cl**:

^{1}H NMR (400 MHz, $CDCl_3$, δ in ppm): δ = 8.39 (s, 1H, -CH=N-), 8.19 (dd, 2H, *J* = 4.0, 8.0 Hz, Ar-H), 8.03 (d, 2H, *J* = 8.0 Hz, Ar-H), 7.98 (d, 1H, *J* = 8.0 Hz, Ar-H), 7.43 (dd, 2H, *J* = 2.2, 6.6 Hz, Ar-H), 7.39-7.35 (m, 3H, Ar-H), 7.22 (dd, 2H, *J* = 2.2, 6.6 Hz, Ar-H), 7.17 (d, 1H, *J* = 8.0 Hz, Ar-H), 7.01 (d, 2H, *J* = 8.0 Hz, Ar-H), 4.08 (t, 2H, *J* = 6.0 Hz, -OCH_2-), 2.68 (s, 3H, -CH_3), 1.89-1.82 (m, 2H, -CH_2-), 1.54-1.47 (m, 2H, -CH_2-), 1.38-1.31 (m, 12H, -$(CH_2)_6$-), 0.91 (t, 3H, *J* = 6.0 Hz, -CH_3).

^{13}C NMR (100 MHz, $CDCl_3$, δ in ppm): δ = 14.14, 15.36, 22.71, 26.00, 29.11, 29.33, 29.38, 29.57, 29.58, 31.91, 68.39, 114.39, 114.44, 122.35, 122.40, 123.21, 126.41, 129.52, 129.56, 130.13, 131.26, 132.39, 132.44, 133.66, 134.57, 149.42, 152.49, 153.72, 159.41, 163.75, 164.62, 166.34.

FT-IR (cm^{-1}): HC=N stretching of an imine at 1609 cm^{-1}, C=O stretching band of ester at 1731 cm^{-1}, C-H stretching of alkanes at 2923 cm^{-1}

UV-vis (nm): 276 nm, 330 nm.

Compound	M+H	M-H	Exact Mass	Observed Mass	% error
10/Cl	626.2673	624.2517	625.2595	626.2643	0.000479

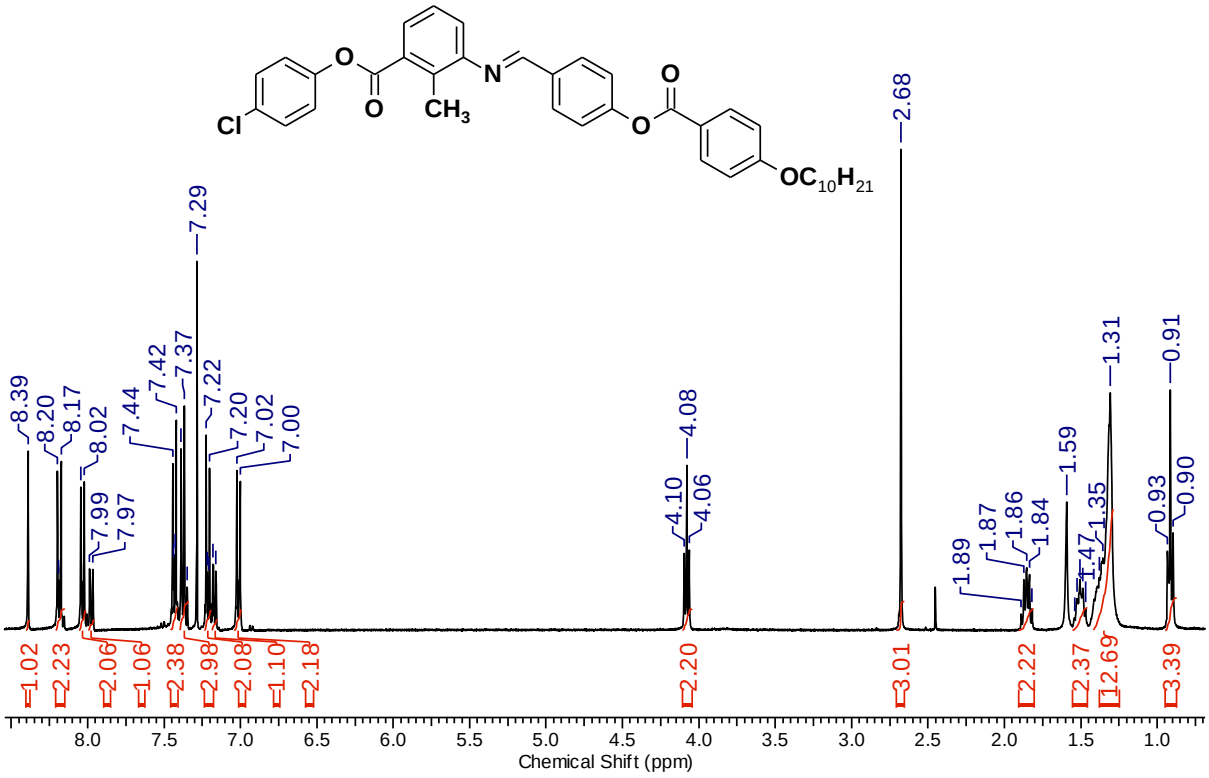

Figure S28: ^{1}H NMR of compound **10/Cl**.

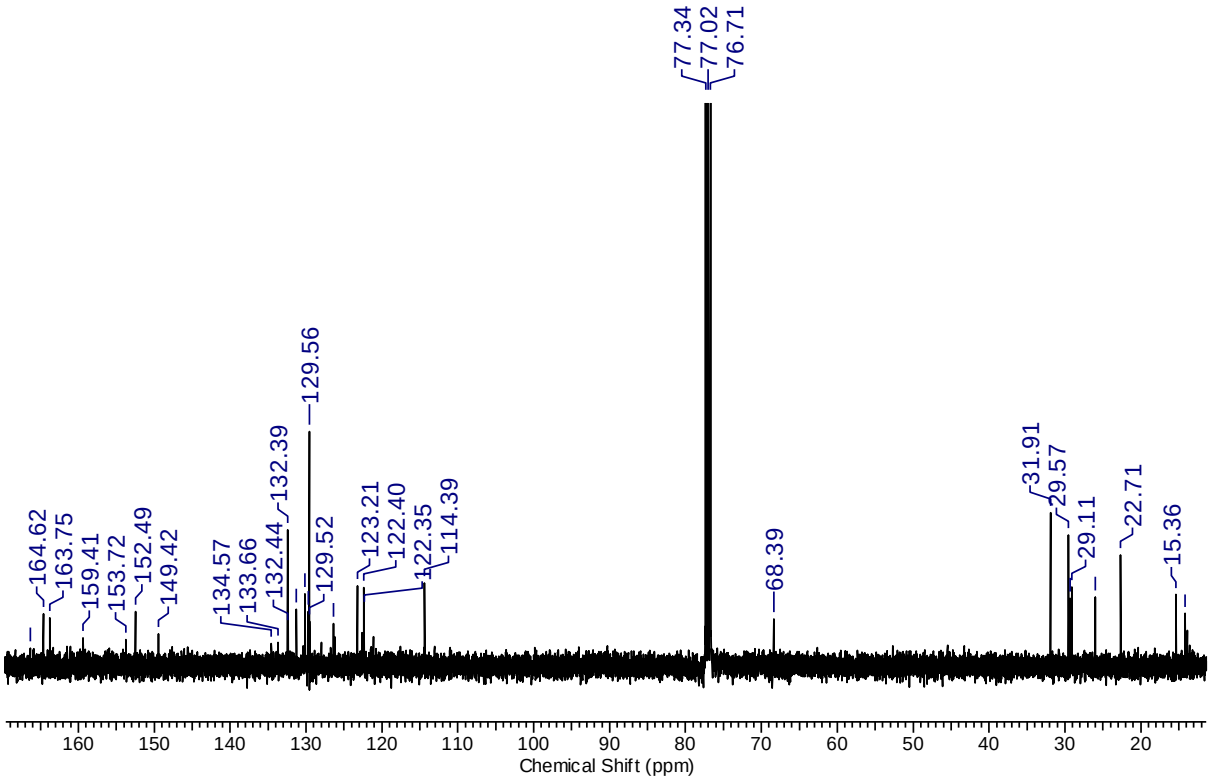

Figure S29: ^{13}C NMR of compound **10/Cl**.

Compound **10/Br**:

^{1}H NMR (400 MHz, $CDCl_3$, δ in ppm): δ = 8.39 (s, 1H, -CH=N-), 8.18 (dd, 2H, *J* = 4.0, 8.0 Hz, Ar-H), 8.03 (dd, 2H, *J* = 1.8, 6.7 Hz, Ar-H), 7.98 (dd, 1H, *J* = 1.0, 7.8 Hz, Ar-H), 7.58 (dd, 2H, *J* = 2.2, 6.6 Hz, Ar-H), 7.39-7.35 (m, 3H, Ar-H), 7.18-7.15 (m, 3H, Ar-H), 7.01 (dd, 2H, *J* = 2.0, 7.1 Hz, Ar-H), 4.08 (t, 2H, *J* = 6.0 Hz, -OCH_2-), 2.67 (s, 3H, -CH_3), 1.89-1.82 (m, 2H, -CH_2-), 1.54-1.47 (m, 2H, -CH_2-), 1.41-1.31 (m, 12H, -$(CH_2)_6$-), 0.91 (t, 3H, *J* = 6.0 Hz, -CH_3).

^{13}C NMR (100 MHz, $CDCl_3$, δ in ppm): δ = 14.15, 15.37, 22.71, 26.00, 29.11, 29.34, 29.38, 29.58, 31.91, 68.40, 114.39, 118.96, 121.12, 122.37, 122.40, 123.64, 126.41, 127.98, 129.67, 130.13, 132.40, 132.55, 133.65, 134.59, 149.97, 150.83, 152.49, 153.72,_159.42, 163.75, 164.63, 165.64.

FT-IR (cm^{-1}): HC=N stretching of an imine at 1605 cm^{-1}, C=O stretching band of ester at 1732 cm^{-1}, C-H stretching of alkanes at 2922 cm^{-1}

UV-vis (nm): 276 nm, 330 nm.

Compound	**M+H**	**M-H**	**Exact Mass**	**Observed Mass**	**% error**
10/Br	670.2168	668.2012	669.2090	670.2144	0.000358

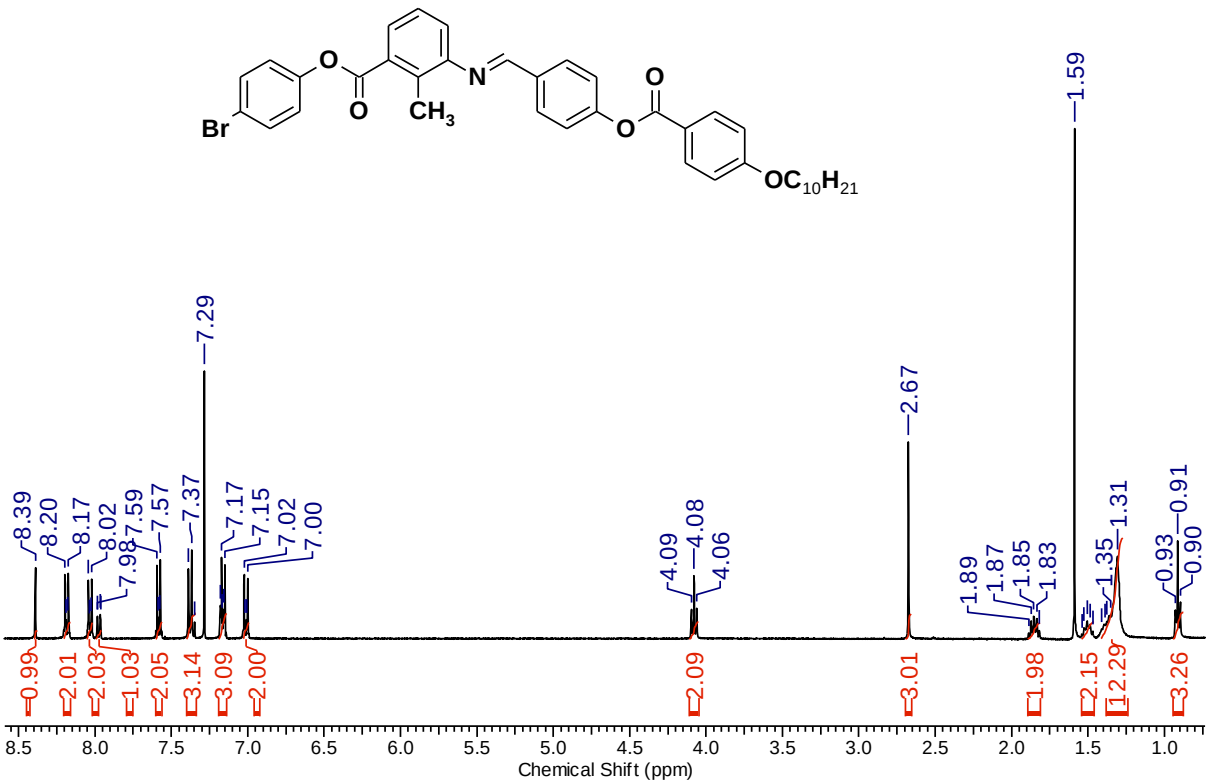

Figure S30: ^{1}H NMR of compound **10/Br**.

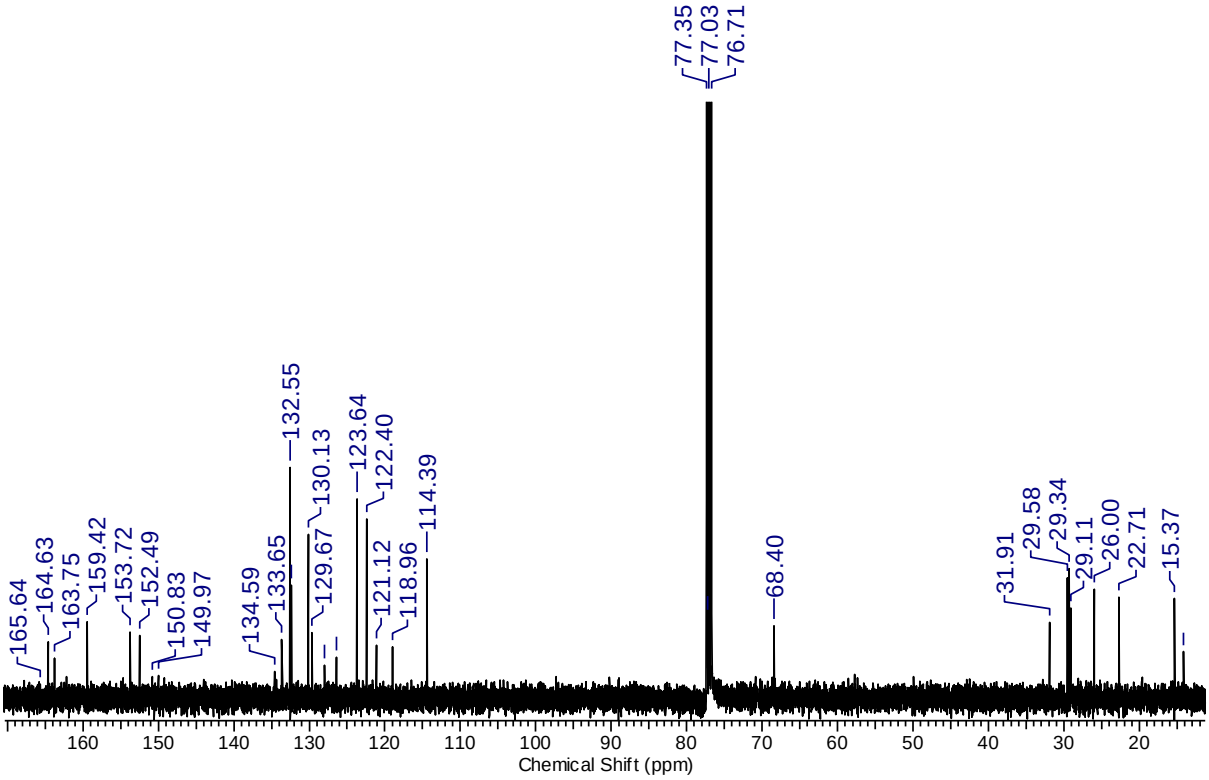

Figure S31: ^{13}C NMR of compound **10/Br**.

Compound **10/I**:

^{1}H NMR (400 MHz, $CDCl_3$, δ in ppm): δ = 8.39 (s, 1H, -CH=N-), 8.18 (d, 2H, *J* = 8.0 Hz, Ar-H), 8.03 (d, 2H, *J* = 8.0 Hz, Ar-H), 7.97 (d, 1H, *J* = 8.0 Hz, Ar-H), 7.77 (d, 2H, *J* = 8.0 Hz, Ar-H), 7.39-7.34 (m, 3H, Ar-H), 7.17 (d, 1H, *J* = 8.0 Hz, Ar-H), 7.05-7.00 (m, 4H, Ar-H), 4.08 (t, 2H, *J* = 6.0 Hz, -OCH_2-), 2.67 (s, 3H, -CH_3), 1.89-1.82 (m, 2H, -CH_2-), 1.53-1.47 (m, 2H, -CH_2-), 1.42-1.31 (m, 12H, -$(CH_2)_6$-), 0.91 (t, 3H, *J* = 6.6 Hz, -CH_3).

^{13}C NMR (100 MHz, $CDCl_3$, δ in ppm): 14.16, 15.40, 22.72, 26.00, 29.11, 29.35, 29.39, 29.59, 31.93, 54.59, 89.91, 114.40, 121.12, 122.42, 124.06, 126.43, 128.00, 129.66, 130.15, 132.41, 133.67, 134.62, 138.57, 147.56, 150.81, 152.50, 153.73, 159.44, 163.77, 164.66, 165.76, 176.26.

FT-IR (cm^{-1}): HC=N stretching of an imine at 1604 cm^{-1}, C=O stretching band of ester at 1732 cm^{-1}, C-H stretching of alkanes at 2922 cm^{-1}

UV-vis (nm): 276 nm, 330 nm.

Compound	M+H	M-H	Exact Mass	Observed Mass	% error
10/I	718.6402	716.6246	717.1951	718.6380	0.000306

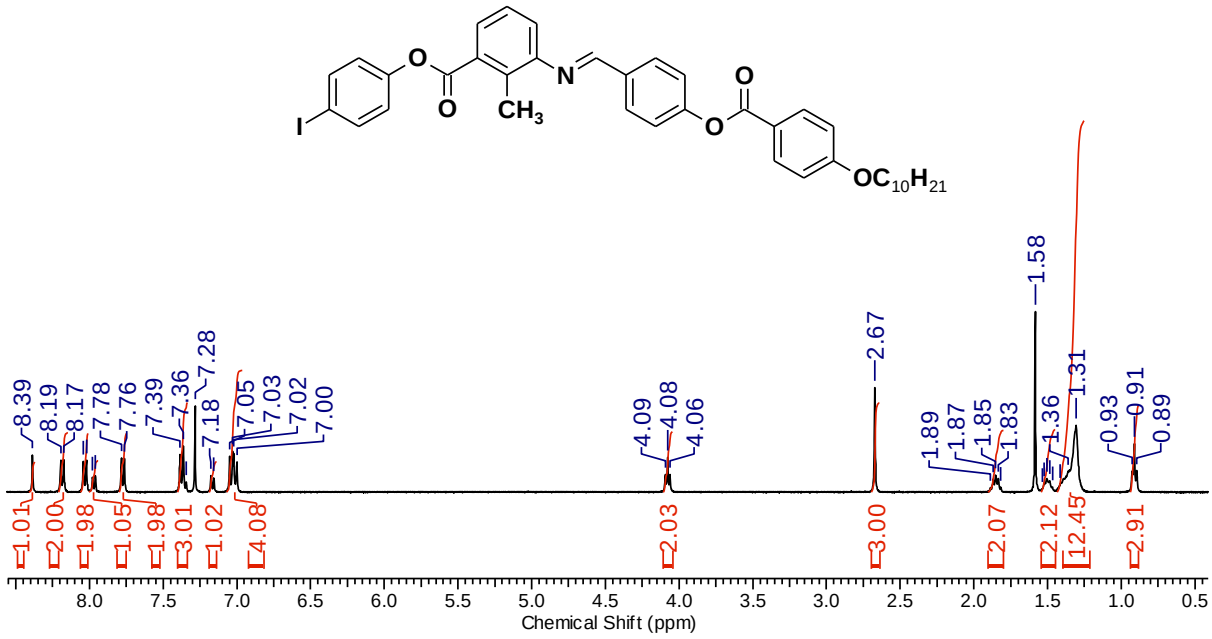

Figure S32: ^{1}H NMR of compound **10/I**.

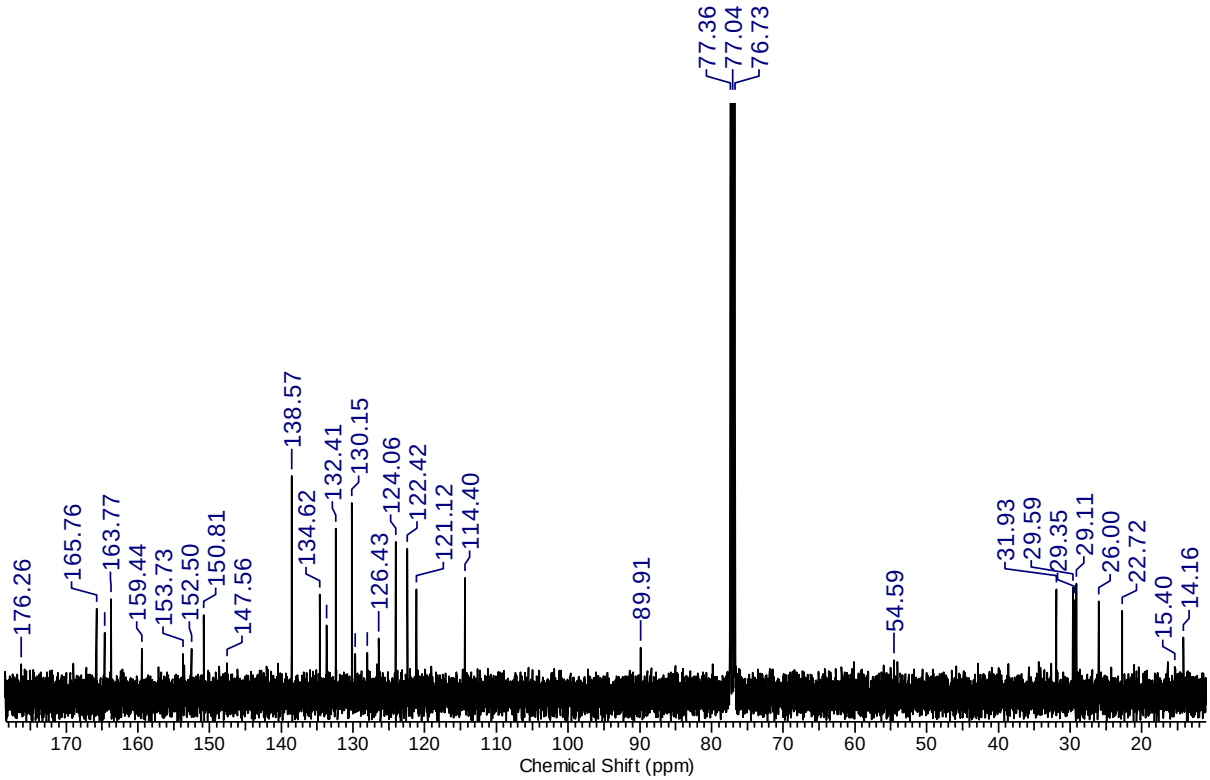

Figure S33: ^{13}C NMR of compound **10/I**.

2. UV-visible studies:

To obtain the information regarding absorption maxima, the UV absorption spectroscopic studies were carried out on one of the series of compounds i.e. **8/X** (X=F, Cl, Br, I) in chloroform solution of c = 1X10^{-4} M concentration. All the compounds exhibited UV absorptions with maximum absorption peak at 276 nm (3.65 eV, ε ~ 41,000 L mol^{-1} cm^{-1}) and a minimum at 330 nm (Figure S34a). The absorption band with large molar absorption coefficient (λ_{max}= 276 nm) corresponds to the π-π* transition basically contributed from the **4-n** intermediate series with a slight red shift. The band at 330 nm reflects the π-π* transition of the highly π-conjugated system with substituted phenyl benzoate unit as the core contributed from the **7X** intermediate series with a slight red shift (Figure S34b). Similar result with absorption maxima 276 nm was found for other homologous series (**6/X** and **10/X**).

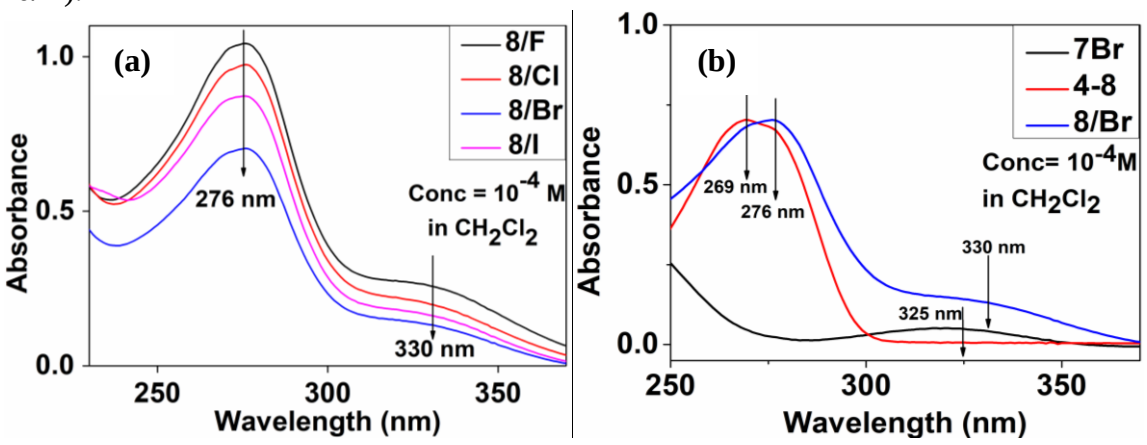

Figure S34: (a) UV-visible spectrum of **8/X** series, (b) Comparative UV-visible plot of the intermediates (**7Br** and **4-8**) and the final compound **8/Br**.

3. Polarising Optical Microscopy:

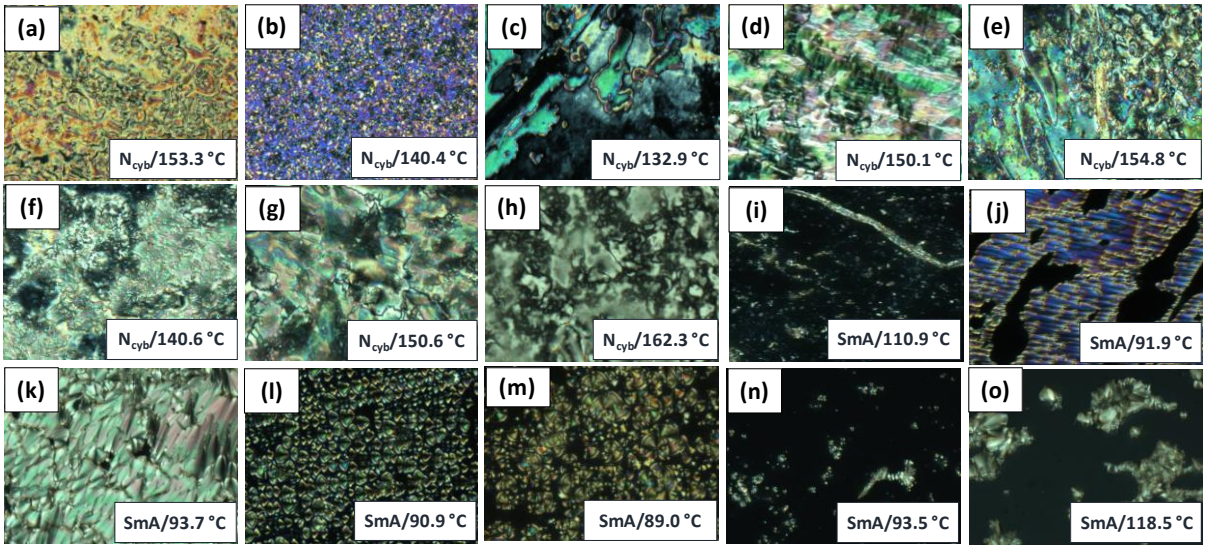

Figure S35: Optical textures observed by POM in the cooling cycle (rate: 10 °C min^{-1}) for all the synthesised compounds (between crossed polariser and analyser); (a) **8/Cl** (b) **8/Br** (c) **6/F** (d) **10/Cl** (e) **6/Br** (f) **8/I** (g) **6/I** (h) **10/I** showing N phase and (i) **8/I** (j) **10/F** (k) **10/Cl** (l) **6/Br** (m) **8/Br** (n) **6/I** (o) **10/I** showing SmA phase.

4. Differential Scanning Calorimetry:

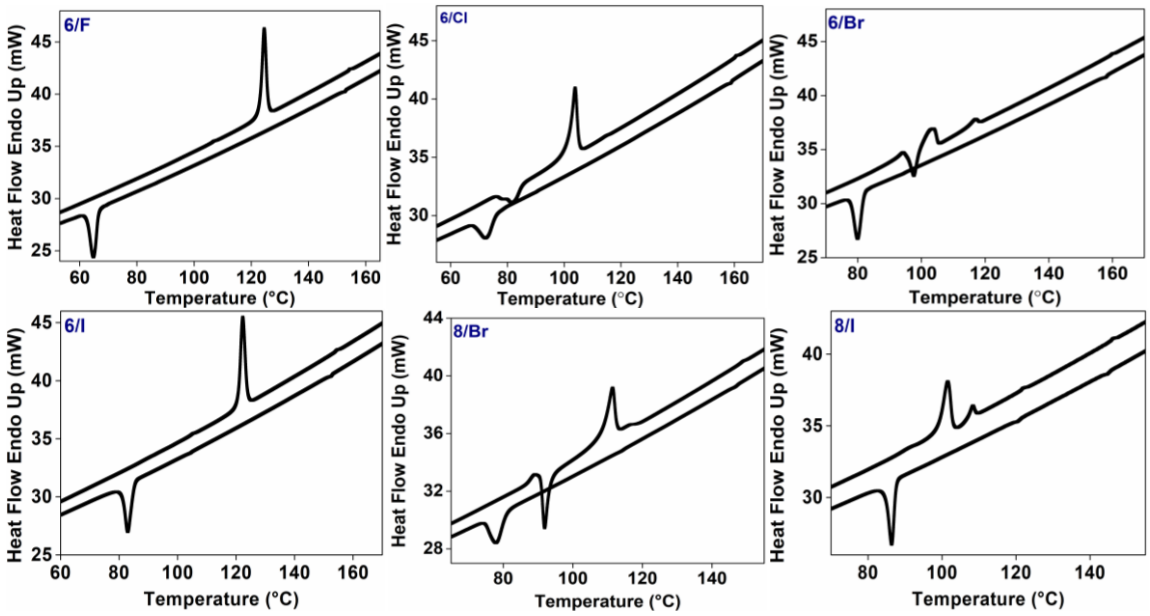

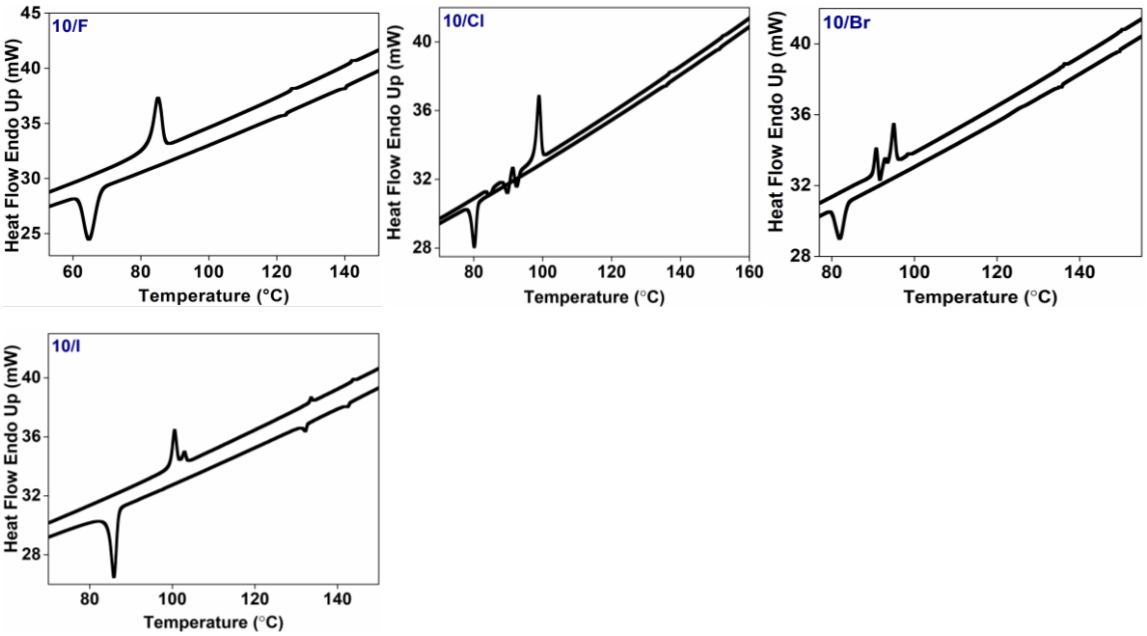

Figure S36: DSC thermograms (both heating and cooling cycles) of the final compounds recorded at 10 °C min^{-1}.

5. X-ray Diffraction studies:

Table S1: Record of intensity ratio of the small-angle peak of **8/F** depicting cybotactic clustering in the N phase with decreasing temperature.

Compound	Temperature (°C)	I_{saxs}	I_{waxs}	I_{saxs}/I_{waxs}
8/F	130	114	115	0.99
	125	128	117	1.09
	120	140	117	1.20
	115	168	119	1.41

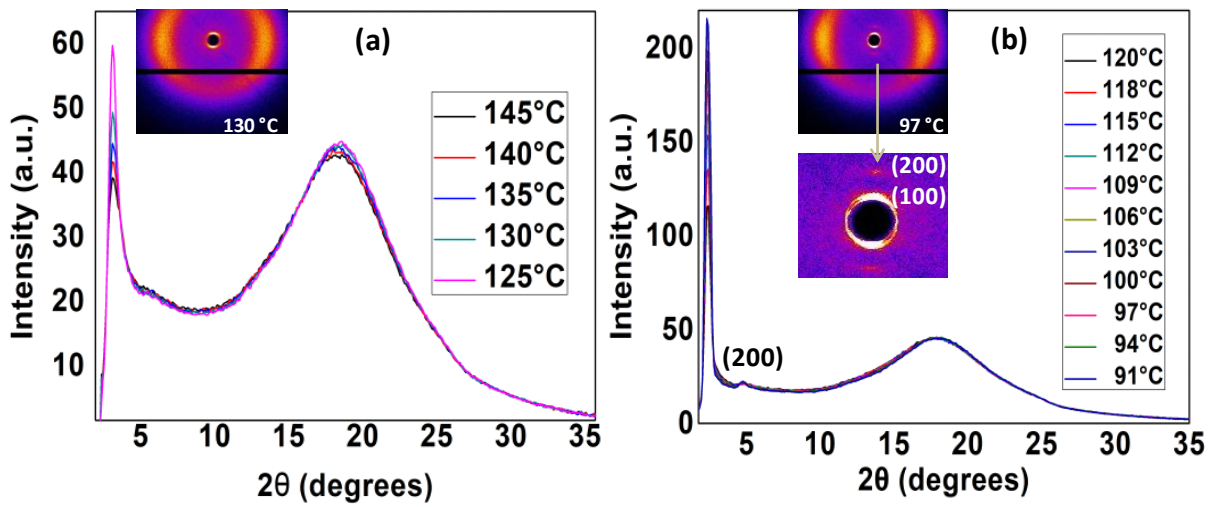

Figure S37: Comparative plot of Intensity vs 2θ in the wide-angle region of **8/Cl** at different temperatures in the (a) N and (b) SmA phase.

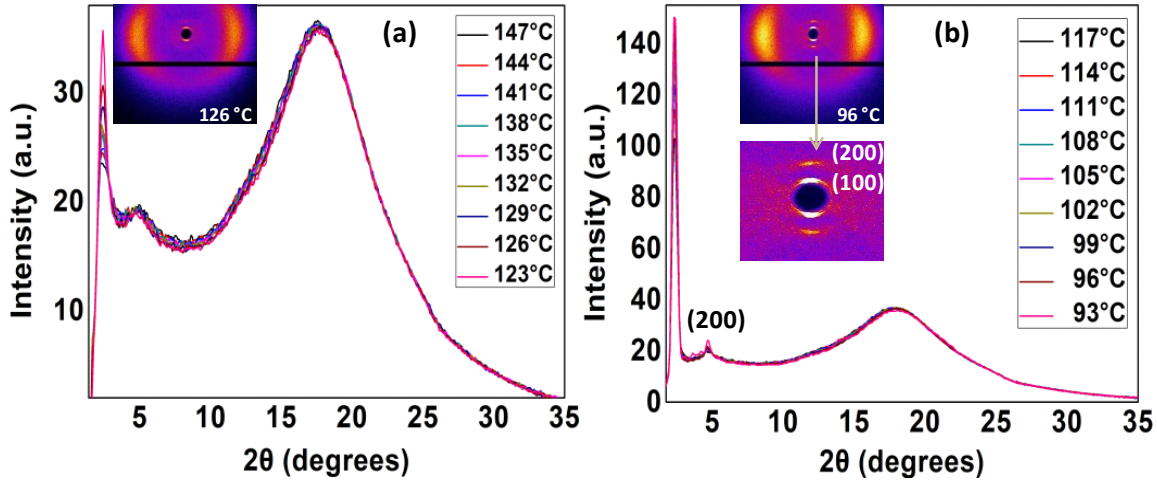

Figure S38: Comparative plot of Intensity vs 2θ in the wide-angle region of **8/Br** at different temperatures in the (a) N and (b) SmA phase.

It has to be noted that there are two peaks or d-spacings present in the low-angle region in ratio ~1:2 in the XRD pattern of **8/Cl** and **8/Br** (Figure S37, S38).[1]

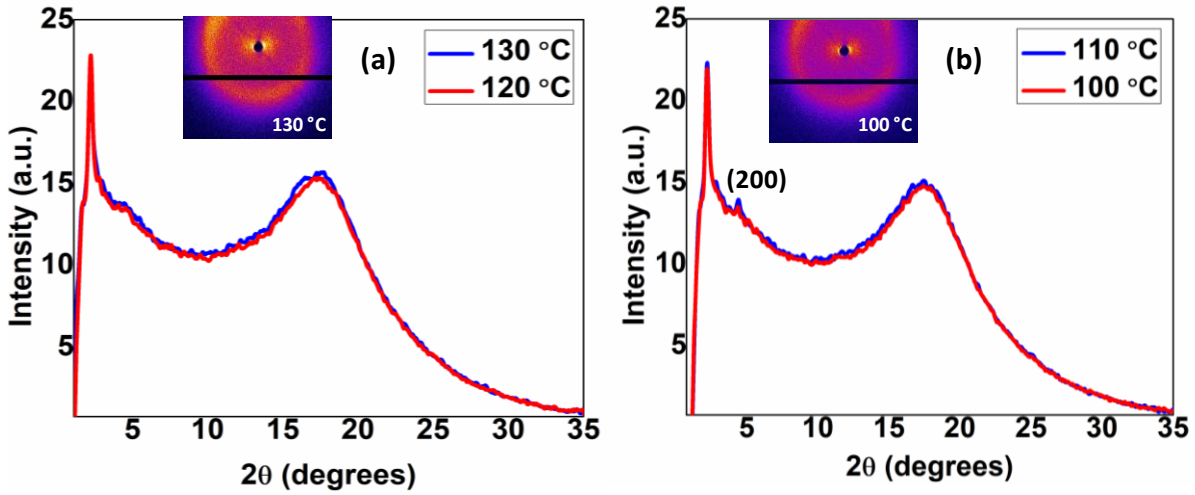

Figure S39: Plot of Intensity vs 2θ in the wide-angle region of **10/I** at different temperatures in the (a) N and (b) SmA phase.

Anomalous behaviour of n/I series:

It was observed that the intensity and sharpness of N and SmA phase peak for **10/I** is almost the same and corresponds to (100) plane. Also, there is a second order reflection (200) in the mid-angle region in the temperature range of SmA phase at d ~ 20 Å (2θ ~ 4.5°) for exposure time 300 s. In case of **6/I** and **8/I**, the two phases are not observed clearly (similar to isotropic) even for the exposure time 1800 s whereas Cr phase is clearly evident. However, the distinction between the two phases i.e. N and SmA has been made successfully with the

help of POM and DSC studies for all the homologues of **n/I** series. This anomalous behaviour in the XRD studies of **n/I** series could be due to the absorption by the heavy atom iodine incorporated in the bent structure.[2]

Therefore, XRD of **n/I** compounds need more detailed investigation as there are limited reports on iodo-containing compounds in bent-core family of compounds.

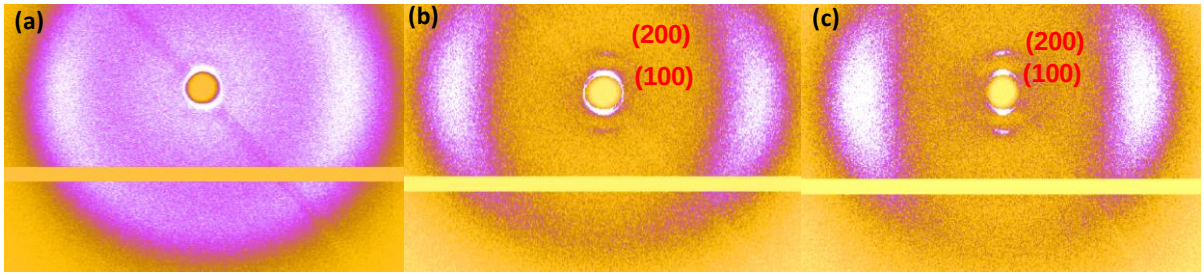

Figure S40: Zoomed portion of 2D X-ray diffraction pattern of the small-angle regime with indexing part of (a) **8/F**, (b) **8/Cl** and (c) **8/Br** recorded at 100 °C of SmA phase.

As the size of halogen increases (F to Br), the second order reflection becomes more distinct.

Table S2: Comparative data of *d*-spacings of the **n/Cl** series in the Sm A phase (at 100 °C) and N phase (at 135 °C).

Compound	**Planes *(hkl)***	**d-spacing (SmA phase)**	**d-spacing (N phase)**
6/Cl	100 200	34.83 17.39 4.95	32.88 16.85 5.02
8/Cl	100 200	37.71 18.48 4.96	35.80 17.39 5.02
10/Cl	100 200	40.23 20.46 4.92	39.17 19.61 5.02

Correlation length (ξ): The correlation length (ξ), that is, the degree of order within the meshophases was calculated using the relation $\xi = [k\ 2\pi]/[(\Delta q)]$ which is equivalent to Scherrer's equation, $\xi = [k\ \lambda]/[(\Delta 2\theta)Cos\theta]$, where, k is the shape factor whose typical value is 1, λ is the wavelength of the incident X-ray, $\Delta 2\theta$ is the broadening in 2θ at half the maximum intensity (FWHM) in radian unit, and θ is the maximum of the reflection. q is the scattering vector ($q=4\pi Sin\theta/\lambda$) and Δq is the broadening in q at half the maximum intensity.

$\Delta q$is obtained by Lorentzian fitting of the peaks obtained in the diffraction pattern. Further, the correlation length of peak divided by corresponding *d*-spacing gives the number of correlated units (n), i.e. it express how many units of that length scale are *tune in on* to show that correlation length. For both **8/Cl** and **8/Br**, correlation length is inversely proportional to temperature. But as temperature is lowered, d-spacing increases for **8/Cl** and decrease for **8/Br**.

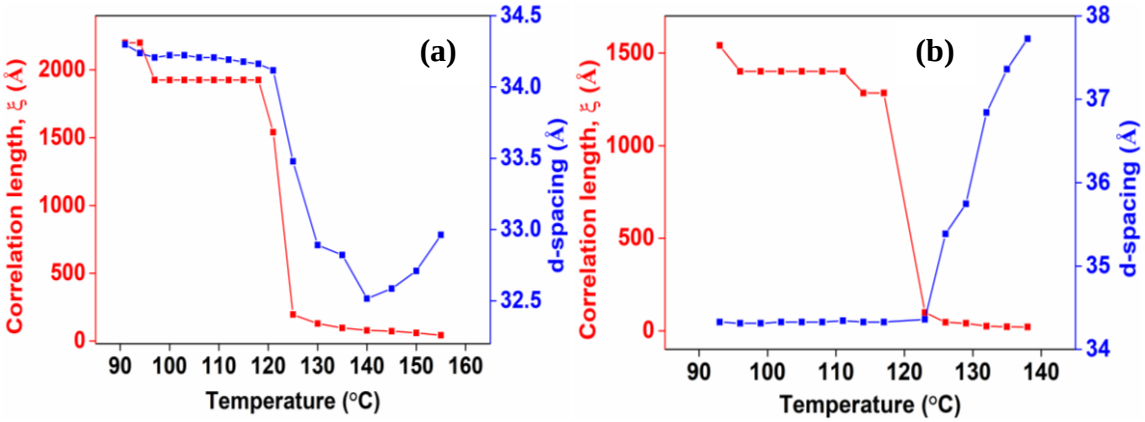

Figure S41: Variation of correlation length (ξ) and *d*-spacing vs Temperature for (a) **8/Cl** and (b) **8/Br**.

6. Temperature dependent Raman study:

Table S3: Vibrational assignment of some experimentally observed Raman bands at room temperature of **8/X** series (X= I, Br, Cl, F).

S. No.	I	Br	Cl	F	Assignment[a]
1	1742	1739	1742	1744	ν(C=O) (terminal ester at long arm)
2	1726	1725	1724	1724	ν(C=O) (central ester at short arm)
3	1639	1639	1639	1635	ν(C=N)
4	1603	1603	1602	1605	ν(C=C) (Phenyl rings)
5	1582	1583	1582	1583	ν(C=C) (Phenyl rings)
6	1455	1455	1455	1456	S (CH_2) (terminal chains)
7	1420	1420	1419	1418	W (CH_3) (central)
8	1258	1260	1258	1260	ν(C-C) (linking group)
9	1219	1220	1220	1223	ν(C-C) (linking group)
10	1201	1200	1200	1199	ν(C-O) (linking group)
11	1175	1175	1175	1177	$\beta_{IN}(C_{32}H_{36})$ (Phenyl rings)
12	1164	1164	1164	1163	$\beta_{IN}(C_{32}H_{36})$ (Phenyl rings)
13	1057	1070	1088	1097	ν(C-X)
14	-	605	653	740	β_{IN} (C-X)

[a]ν: stretching, β: bending, S: scissoring, W: wagging, IN: in plane, X= I, Br, Cl, I.

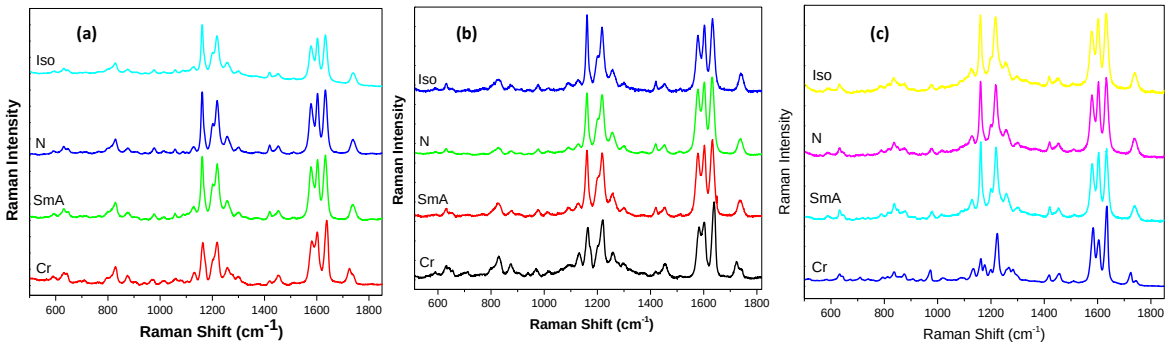

Figure S42: Temperature dependent Raman spectra at different temperature in the range 500-1800 cm^{-1} for (a) **8/I**, (b) **8/Cl** and (c) **8/F**.

7. DFT Studies:

All computations were performed with the Gaussian 09 and GaussView 5.0 package. DFT calculations with the B3LYP functional and the 6-311G (d, p) basis set were carried out to optimize the geometry of the compounds with F, Cl, Br terminal group while for the I-compounds 6-31G (d, p) LanL2DZ basis set was used. All geometry optimization was accompanied by frequency analyses; the absence of negative vibrational frequencies indicated convergence on minimum energy structures.

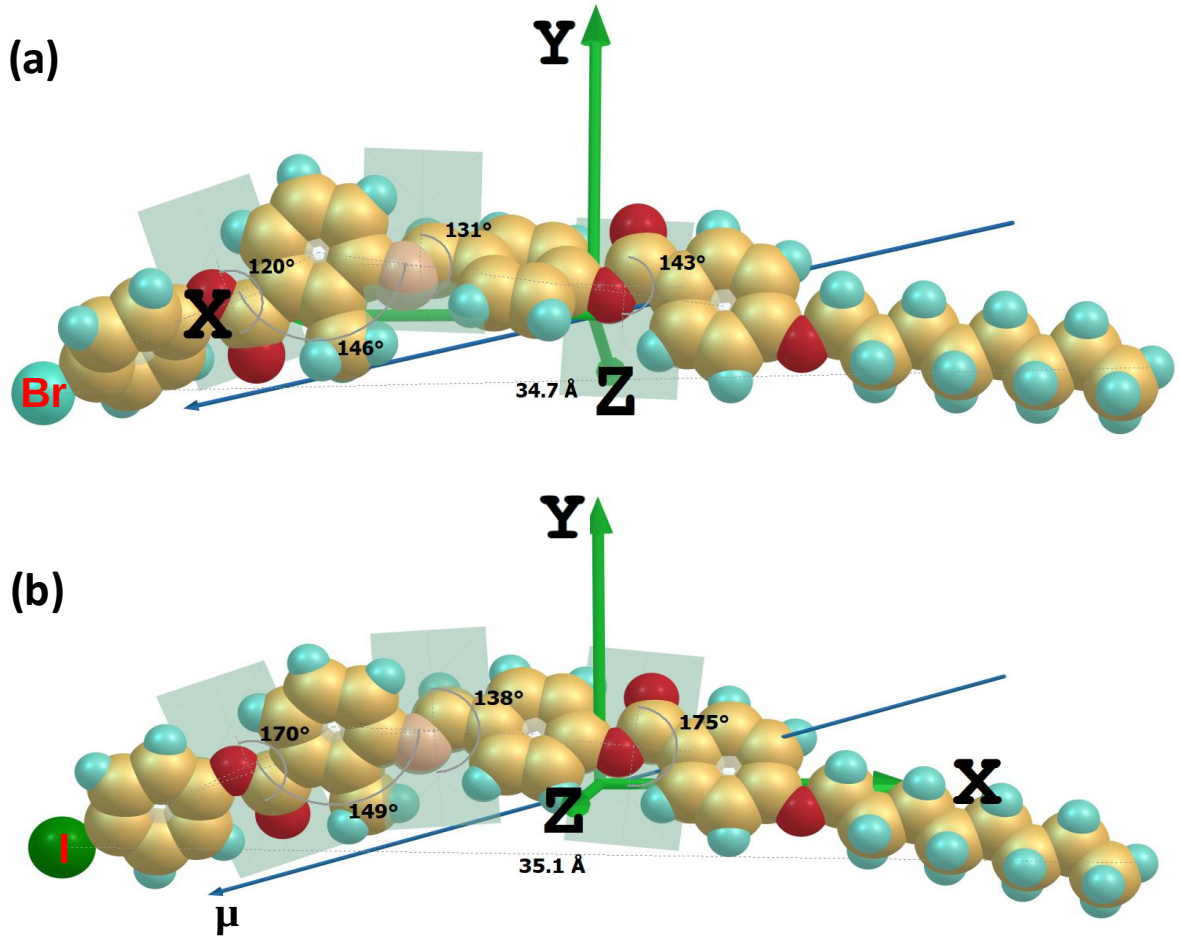

Figure S43: DFT optimised molecular structure of (a) **n/Br** and (b) **n/I** in Cartesian coordinate frame displaying bent angle, dihedral angle, resultant dipole moment direction (μ) and molecular length.

8. Materials and reagents:

All chemicals and solvents were all of AR quality and were used without further purification. 4-Hydroxybenzaldehyde, 3-Amino-2-methylbenzoic acid, 4-Fluorophenol, 4-Chlorophenol, 4-Bromophenol and 4-Iodophenol were all purchased from TCI (Japan); N, N-Dicyclohexylcarbodiimide (DCC) from Fluka Analytical; 4-Dimethylaminopyridine (DMAP) and potassium hydroxide from Sigma Aldrich; 4-Hydroxybenzoic acid from Himedia. Column chromatographic separations were performed on silica gel (100-200 mesh). Thin

layer chromatography (TLC) was performed on aluminium sheets pre-coated with silica gel (Merck, Kiesegel 60, F254).

9. Instrumental:

Structural characterisation of the compounds was carried out with a combination of FT-IR (Infrared Spectroscopy-Perkin Elmer Spectrum AX3), UV-VIS-NIR spectrophotometer (LABINDIA UV-Vis Spectrophotometer 3000+), High Resolution Mass Spectrometry (Waters synapt g2s), ^{1}H-NMR and ^{13}C-NMR (BrukerBiospin Switzerland Avance-iii 400 MHz and 100 MHz spectrometers respectively). NMR spectra were recorded using deuterated chloroform ($CDCl_3$) as solvent and tetramethylsilane (TMS) as an internal standard. Polarising Optical Microscopy (POM) textural observations of the mesophases were performed with Nikon Eclipse LV100POL polarising microscope provided with a Linkam heating stage (LTS 420) and the images were captured using a Q-imaging camera. Differential Scanning Calorimetry (DSC) measurements were performed on Perkin Elmer DSC 8000 coupled to a Controlled Nitrogen Accessory (CLN2) with a scan rate of 10 ˚C min^{-1} both on heating and cooling. X-ray Diffraction (XRD) studies were carried out on samples using CuKα (λ=1.54 Å) radiation from GeniX3D microsource operating at 50kV and 0.6 mA, using Pilatus 200K detector in Xeuss 2.0 SAXS/WAXS system.

10. References:

1 A. K. Yadav, B. Pradhan, H. Ulla, S. Nath, J. De, S. K. Pal, S. M. N and A. Ammathnadu Sudhakar, *J. Mater. Chem. C*, 2017, DOI: 10.1039/C7TC01420A.

2 M. Alaasar, M. Prehm and C. Tschierske, *Chem. Commun.*, 2013, **49**, 11062-11064.